LITHIUM SULPHATE-BASED SOLID ELECTROLYTES FOR ADVANCED BATTERIES

by

A. V. N. TILAK

TH
IPMS/1984/M
T45L

INTERDISCIPLINARY PROGRAMME IN MATERIALS SCIENCE
INDIAN INSTITUTE OF TECHNOLOGY, KANPUR
AUGUST 1984

LITHIUM SULPHATE-BASED SOLID ELECTROLYTES FOR ADVANCED BATTERIES

A thesis submitted
in Partial Fulfilment of the Requirements
for the degree of

MASTER OF TECHNOLOGY

T 30 P

by

A. V. N. TILAK

to the

INTERDISCIPLINARY PROGRAMME IN MATERIALS SCIENCE
INDIAN INSTITUTE OF TECHNOLOGY, KANPUR

AUGUST 1984

83987

MS-1984-M-TIL-LIT

POST GRADUATE OFFICE
Submitted on.....

CERTIFICATE

Certified that this work on "Lithium Sulphate-based Solid Electrolytes for Advanced Batteries" by A.V.N. Tilak has been carried out under my supervision and that this has not been submitted elsewhere for a degree.

(Dr. K. Shahi)
Assistant Professor
Materials Science Programmme
Indian Institute of Technology,
Kanpur.

POST GRADUATE OFFICE
This thesis has been approved
for the award of the Degree of
Master of Technology (M.Tech.)
in accordance with the
regulations of the Indian
Institute of Technology,
Kanpur.
Dated. 26/8/04

ACKNOWLEDGEMENTS

The author is deeply indebted to Dr. K. Shahi who introduced him to the subject. It was great pleasure for the author to work with him as both freedom of work and necessary guidance in addition to training were available. The author is grateful to him for his meticulous guidance throughout the work.

The author would like to thank Messers B.Sharma & A.N. Prasad for their invaluable help during the various phases of experimental work.

The excellent typing by Mr. Jawar Singh and the careful duplicating work of Mr. Vishwanath Singh is very much appreciated.

Finally the author would like to thank his friends K.N.Rao, K. Sudhakar, R.V. Gopal and N. Siva Prasad for their timely help.

CONTENTS

CHAPTER		PAGE
	LIST OF FIGURES	iii
	LIST OF TABLES	v
	ABSTRACT	vi
1.	INTRODUCTION	1
	1.1. Solid Electrolytes	2
	1.1.1. Historical Background	3
	1.1.2 General Properties and Theoritical Aspects	7
	1.1.3 General Applications of Solid Electrolytes	17
	1.2 Role of Li and Na ion Conductors	22
	1.3 Advanced Solid Electrolyte Batteries	26
	1.3.1 Present Status and The Statement of the Problem	29
2.	EXPERIMENTAL TECHNIQUES	
	2.1 Introduction	32
	2.2 Starting Materials	33
	2.3 Preparation of Pellets	34
	2.4 Measurement Techniques	39
3.	RESULTS AND DISCUSSION	
	3.1 Starting Materials	45
	3.1.1. Lithium Sulphate	45
	3.1.2. Lithium Chloride	58
	3.2 Li_2SO_4-LiCl Composites	61
	3.3. Li_2SO_4-LiCl-Al_2O_3 System	77
	3.4 Summary and Conclusions	81
	REFERENCES	84

--

LIST OF FIGURES

FIGURE		PAGE
1.1	Electrical conductivity as a function of temperature for various solid electrolytes	10
1.2	Electrical conductivity as a function of temperature for various sodium ion conductors	24
1.3	Electrical conductivity variation of various lithium ion conductors with temperature	24
2.1	Stainless-steel die for making pellets	38
2.2	Sample holder for the electrical conductivity measurements	40
2.3	Block-diagram connections for electrical conductivity measurements	42
3.1	Electrical conductivity of pure Li_2SO_4 as a function of temperature	48
3.2	Electrical conductivity of 10 mole% LiCl as a function of temperature	57
3.3	Electrical conductivity of pure LiCl as a function of temperature	60
3.4	Electrical conductivity variation of Li_2SO_4-LiCl system with composition at three different temperatures	62
3.5	The phase diagram of the system Li_2SO_4-Li_2Cl_2	64
3.6	Electrical conductivity variation of various compositions of Li_2SO_4-LiCl with temperature	66

3.7 Electrical conductivity variation of dd compositions of Li_2SO_4-LiCl with temperature 67

3.8 Electrical conductivity variation of even compositions of Li_2SO_4-LiCl with temperature 68

3.9 Electrical conductivity of 20 mole % LiCl as a function of temperature 71

3.10 Electrical conductivity of 30 mole % LiCl as function of temperature 72

3.11 Electrical conductivity of 40 mole % LiCl as function of temperature 74

3.12 Electrical conductivity of 50 mole % LiCl as function of temperature 75

3.13 Electrical conductivity of 60 mole % LiCl as function of temperature 76

3.14 Electrical conductivity of 70 mole % LiCl as function of temperature 78

3.15 Electrical conductivity of 80 mole % LiCl as function of temperature 79

3.16 Electrical conductivity of 90 mole % LiCl as function of temperature 80

3.17 Electrical conductivity variation of Li_2SO_4+30 % LiCl+ 30 % Al_2O_3 with temperature 82

LIST OF TABLES

TABLE		PAGE
1.1	Electrical conductivity of various substances at room temperature	9
1.2	Ionic conductivity of various sodium ion conductors at room temperature	23
1.3	Ionic conductivity of some selected Li^+-based fast ion conductors	26
1.4	Performance figures of various energy storage batteries	28
1.5	OCV and energy density of various Li - batteries	29
1.6	Performance characteristics of some commercial solid electrolyte lithium batteries	31
2.1	Chemical analysis of $Li_2SO_4.H_2O$	34
2.2	Chemical analysis of LiCl	35
2.3	Characteristics of Li_2SO_4 and LiCl	36
3.1	Activation energies and pre-exponential factors for Li_2SO_4-LiCl system	50

--

LIST OF TABLES

TABLE		PAGE
1.1	Electrical conductivity of various substances at room temperature	9
1.2	Ionic conductivity of various sodium ion conductors at room temperature	23
1.3	Ionic conductivity of some selected Li^+-based fast ion conductors	26
1.4	Performance figures of various energy storage batteries	28
1.5	OCV and energy density of various Li - batteries	29
1.6	Performance characteristics of some commercial solid electrolyte lithium batteries	31
2.1	Chemical analysis of $Li_2SO_4.H_2O$	34
2.2	Chemical analysis of LiCl	35
2.3	Characteristics of Li_2SO_4 and LiCl	36
3.1	Activation energies and pre-exponential factors for Li_2SO_4-LiCl system	50

--

ABSTRACT

With a view to improving the electrical conductivity of lithium sulphate at the lowest possible temperature, LiCl was added in the ratios of 10-90 mole% and its conductivity was measured. The low temperature phase of Li_2SO_4 (i.e. β-Li_2SO_4) containing 50 mole % LiCl has the maximum conductivity, $\sim 5.5 \times 10^{-2}$ ohm^{-1} cm^{-1} at 500°C. With the addition of 50 mole% LiCl, the conductivity of Li_2SO_4 has increased by a factor of 1000 at temperatures of 200-400°C, and by a factor of 50 at temperatures above 400°C.

Deposition of fine Al_2O_3 particles in Li_2SO_4 + 30 mole% LiCl has not shown any further improvement in the electrical conductivity. The conduction parameters (pre-exponential factor and activation energy) for different compositions of Li_2SO_4- xLiC (x=0, 0.1, 0.2, 0.3, 0.4, 0.5, 0.6, 0.7, 0.8, 0.9, 1.0) are calculated from the experimental data and are tabulated.

INTRODUCTION

As the conventional energy sources, such as coal,oil, and natural gas draw. to a close and technology progresses, the search for alternate energy sources increases. While research is going on for developing alternative sources of energy, storing of energy poses another problem. Energy storage is an essential activity in the energy supply system besides exploitation of the resources, conversion and transport. Storage is a necessity for delivering the required energy.

Generally, storage requires investments and is more or less a source of energy losses. For economic usage of conventional power one needs load-leveling which can be obtained utilizing a storage system.

There are several ways of storing electrical energy. The chemical bond represents the most versatile form of energy storage, the energy in a fuel is concentrated and easy to handle. Therefore, secondary batteries-and elecrolysis cells, which convert electrical energy into chemical energy, are natural complements to any scheme for electric-power generation from wind or nuclear or wave power or from sunlight.

The reconversion of chemical energy to electrical energy can, in principle, be accomplished most economically in a battery or fuel cell. However the batteries used till recently have serious limitations as far as their usability is concerned. Typical lead-acid cells or other reversible cells based on liquid electrolytes do not have high power-density or high shelf- and cycle-life or the ruggedness. Also they can not be charged or discharged very quickly,

that is they are inefficient and it is on this account that these liquid electrolyte batteries could not find wide spread industrial applications.

The recent discovery of a new class of materials called superionic conductors or solid electrolytes or fast ion conductors has given a new hope for development of a new generation of advanced, high energy density batteries which can be used not only for domestic applications (e.g. in transistor-radios, calculators, watches, cameras, etc.) but also for industrial applications such as load-leveling, auto-traction, pace makers, etc. These new said materials (Superionic conductors or Fast ion conductors or Solid electrolytes) are exceptionally good ionic conductors at room temperatures and even below, and are inherently superior to liquid electrolytes in as much as they do not require a container, can be prepared in thin film, or tubular on pellet form, etc. In addition, the solid electrolyte batteries have

i) long shelf life (8-10 years)

ii) wide temperature range of operation (-100 to 300°C)

iii) high energy density (100-350 KW/Kg.)

In the present work, an effort is made to develop a new lithium based solid electrolyte material that finds application in devices such as high energy density batteries operated at relatively lower temperatures.

1.1. SOLID ELECTROLYTES

Solid electrolytes or fast ion conductors or more popular superionic conductors are a class of new materials which achieve ionic conductivities comparable with those of molten salts or

liquid electrolytes while still in the solid phase. The electronic conductivity of these materials is negligible. These solid electrolytes are unusual solids in which the regularity of the crystalline lattice is significantly disrupted. Dilute point-defect ionic-solids (e.g., NaCl) have been referred to as solid electrolytes by many investigators. These materials have achieved great interest both for basic scientific studies and for technological applications, e.g., in high energy and power density battery systems, sensors, coulometers, fuel cells, etc.

1.1.1. Historical Background

Solid electrolytes have been known since the nineteenth century. Knowledge of these materials has been collected in a rather arbitrary way, stressing temporarily different materials and aspects. It is only in the last fifteen years that theory and application of solid electrolytes have begun converge into a coherent field.

Most often Faraday is credited with having first observed in 1830 the charge transport via movement of ions. His test sample was "Sulphurate of Silver", i.e. Ag_2S. However, it was not until Kohlrausch (1882) when systematic studies of ionic conduction had begun. Kohlrausch's (1882) test sample was AgI, which by the way is the best superionic conductor even today, and exhibits enough intriguing properties so as to sustain researcher's interest even now. AgI is known since Kohlrausch's (1882) work to have a $\sigma \sim 1$ ohm^{-1} cm^{-1}, at 150°C or 15 orders of magnitude larger than that of NaCl at the same temperature. AgI was extensively used to study the ionic solids and establish the general laws those applied to solid ionic conductors such as Faradays

laws of electrolysis, Gibbs, Helmholtz equation etc. A great deal of study in this connection was carried out by Tubandt and co-workers during 1910-1940, see for example Tubandt (1938). In both AgI and Ag_2S (and of course numerous AgI-based fast ion conductors known today) are pure Ag^+ ion conductors, i.e. the electricity in these solids is exclusively carried by Ag^+ ions, not electrons.

Another early demonstration of electrical charge transport by the motion of ions in solids was employed in a practical broad band light source (Nernst, 1897, 1900, Nernst and wild, 1901, Reynolds, 1902). This device, known as the'Nernst glower' consisted of doped ZrO_2, which conducts electrical charge by the motion of the defects in the oxide ion lattice, A few more compounds with high ionic conductivities were found little later. For example a high ionic conductivity of lithium sulfate was reported in 1921.

All these good ionic conductors, which ofcourse now are known as superionic conductors or Fast ion conductors, were ignored for further studies, and labelled" abnormal Substances ". As a result the mechanism of abnormally high ionic conductivity in some restricted salts was unknown for a long time.

Important progress was made around 1935 when Strock observed that AgI after passing through a phase transition at 147°C reaches an ionic-conducting solid state which persists upto the melting point (555°C). A similar observation was made by Ketelaar (1934) for Ag_2HgI_4, essentially a double salt of $2AgI+HgI_2$, for which the phase transition occurs at 50°C. Yet another example was discovery by Reuter and Hardel (1963,1965) who found that Ag_3SI ($AgI+Ag_2S$) exhibited exceptionally high

conductivity at temperatures greater than 235°C, the critical temperature.

However, the real breakthrough did not came until late 1960s. In 1967, a new family of materials were discovered by scientists at Atomics International having superionic conductivity at temperatures even below room temperature. Owens and Argue (1967) and Bradley and Greene (1966) independently found that MAg_4I_5 (where M=K, Rb,NH_4, etc.) exhibit conductivity of 0.3 $ohm^{-1} cm^{-1}$ at room temperature and that this high conductivity phase persisted down to -155°C. It should be pointed out that MAg_4I_5 was the first family of materials to exhibit such a high conductivity at room temperature and below, i.e. the transition to low conducting phase occurs only at low temperatures. The discovery of MAg_4I_5 family was a real milestone because they offered great potential for application in devices which could operate at room temperature. There is one common feature to all these materials, viz, AgI, Ag_2HgI_4, Ag_3SI, MAg_4I_5 etc., and that is the presence of a phase transition. There is a critical temperature T_c below which the material behaves as a normal ionic conductor, and above T_c it is a fast ion or superionic conductor. This behaviour is often referred to as normal to superionic phase transition, and is present in wide variety of superionic conductors. M_2SO_4(M= Li,Na) also exhibit a similar phase transition. Many of fluorites (e.g., PbF_2,CaF_2 etc.) become fast ion conductors only after passing through a phase transition at high temperatures. The normal to superionic phase transition has emerged as an important area of activity within the broad field of superionic conductors. A number of theories/ models have been proposed to explain this unique phenomenon of

phase transition (Rice et.al., 1974, Huberman, 1974, Shahi and Wagner, 1981).

Incidently, the year 1967 witnessed yet another major discovery of M-β- Al_2O_3 (M= Li,Na,K,Rb,Ag, Tl, etc.) by the scientists of Ford Motor Co. (Yao and Kummer, 1967, Radzilowski, 1969, Kummer, 1972). The family of M-β-Al_2O_3 ion conductors exhibited a conductivity in the range of 10^{-2} to 10^{-3} $ohm^{-1}cm^{-1}$, the maximum conductivity being exhibited by Na-β-Al_2O_3, i.e. when M= Na. It should be mentioned that the term sodium-beta-Alumina is a misnomer. It's actual chemical composition is M_2O : 11 Al_2O_3. The name beta-alumina was given because the earlier scientists thought that it was another polymorph of alumina, and apparantly were unaware of soda (Na_2O) content. In any case it is now well known that M-β-Al_2O_3 (M_2O : 11 Al_2O_3) has altogher different composition, properties and structure. There is one fundamental difference between M-β-Al_2O_3 family and MAg_4I_5 family of fast ion conductors, that is MAg_4I_5 exhibit fast ion conduction at temperatures above a critical temperature T_c, while M-β-Al_2O_3 family does not exhibit such a phase transition. That is in case of M-β-Al_2O_3 there is a single fast ion phase stable over a wide temperature range. It is indeed exceptional that such a massively defective structure is stable over temperatures ranging from very high to very low. Another significance associated with M-β-Al_2O_3 was that it allowed rapid transport of light alkali ions such as Liand Na which give rise to large energy density batteries. In fact, the Ford group (Weber and Kummer, 1967) showed that solid electrolytes such as Na-β-Al_2O_3 could be employed in a radical new design of a secondary battery.

Another major breakthrough was broughtout by Kiukkola and Wagner (1957) who pointed out the potentialities of solid electrolytes for thermodynamic investigations at moderate and high temperatures and reintroduced the calcia-stabilized zirconia (CSZ).

As a result of the attention drawn by such developments, activities in this area have increased rapidly in recent years. In addtion to work on the development of practical devices employing solid ionic conductors as solid electrolytes and various types of electrochemical transducers, growing attention has been given to the many scientific questions relating to the unusual behavior of some of these materials. In the past ten years a large number of new fast ion conductors have been discovered. Majority of these are Ag and Cu ion conductors. Some are Li^+, Na^+, H^+ and F^- ion conductors. O^{--} is the only divalent ion which has been found quite mobile in solid state, for example in Zirconia,. However one of the major activities continues to be the search for new and better fast ion conductors particularly based on Li^+ and Na^+ ion transport.

1.1.2 General Properties and Theoritical Aspects

Solid electrolytes are substances that have a high ionic conductivity, but a negligible electronic conductivity. Most of these materials are as yet restricted to work at elevated temperatures, and much effort is going on to lower the operating temperatures to technically more convenient ranges.

There are several ways of classifying the large number of known solid electrolytes. There are two major groups and they differ by the way in which they achieve their electrical conductivity.

The first group (e.g. β- alumina) is characterized by a gradual change into the conducting state. The second group is characterized by a first-order phase transition to the conducting state. Examples of this group as pointed out earlier, are AgI, Li_2SO_4, etc., which are known to have ionic conductivities in their high temperature phases comparable to those of best liquid electrolytes.

According to the type of substance the solid electrolytes can generally be divided into three catagories. The first catagory inorganic crystalline solids, is by far the largest of solid electrolytes and includes both anion and cation conductors. Anion conductors consist of fluoride oxide ion conductors, whereas the cation conductors consist of alkalimetal, silver and copper ion conductors.

In addition to the anion and cation conductors, recently, some proton conductors have been found to have high ionic conductivities at relatively lower temperatures.

The second catagory consists of glass conductors such as Li^+,Na^+ and Ag^+. Polymeric materials prepared from polythylene and alkali metal salts which show high ionic conductivities comes under the third category. Although the conductivities of glasses and polymers are generally much lower than those of inorganic solids, they have important advantages because of their greater plasticity, isotropic conductivity and absence of grains.

From the point of view of the crystal structure characteristics of the materials, solid electrolytes can be classified into several groups. First group are the materials (e.g. β-alumina) in which the transport takes place along two-dimensional paths. In the second group of materials (e.g. $RbAg_4I_5$) the

transport takes place in a frame work of three-dimensionally cross-linked channels. Except for the fluorite ion conductors, a majority of solid electrolytes known at present have a large ratio of available lattice sites per mobile ion.

Table 1.1 compares the room temperature (25°C) conductivities of different categories of solid electrolytes with conductivities of other substances.

Table 1.1

Type of substance	Substance (Charge carrier)	Conductivity $(\text{ohm.cm})^{-1}$
Metal	Cu (electrons)	10^{6}
Crystalline solid	k β''-alumina (K^+)	10^{-1}
Aqueous solution	0.1M KCl(K^+ and Cl^-)	10^{-2}
Glass	0.75 Ag 0.25 $Ag_2 MoO_4$ (Ag^+)	10^{-2}
Polymer	4.5 Polyethylene Oxide.Na B F_4 (Na^+)	10^{-7}

Fig. 1.1 shows the temperature variation of electrical conductivity for some solid electrolytes.

Two basic features to explain the theory of solid electrolytes are the origin of the formation of the substantial disordering required for the electrolytic conductivity in solid electrolytes and the transport mechanism in such disordered

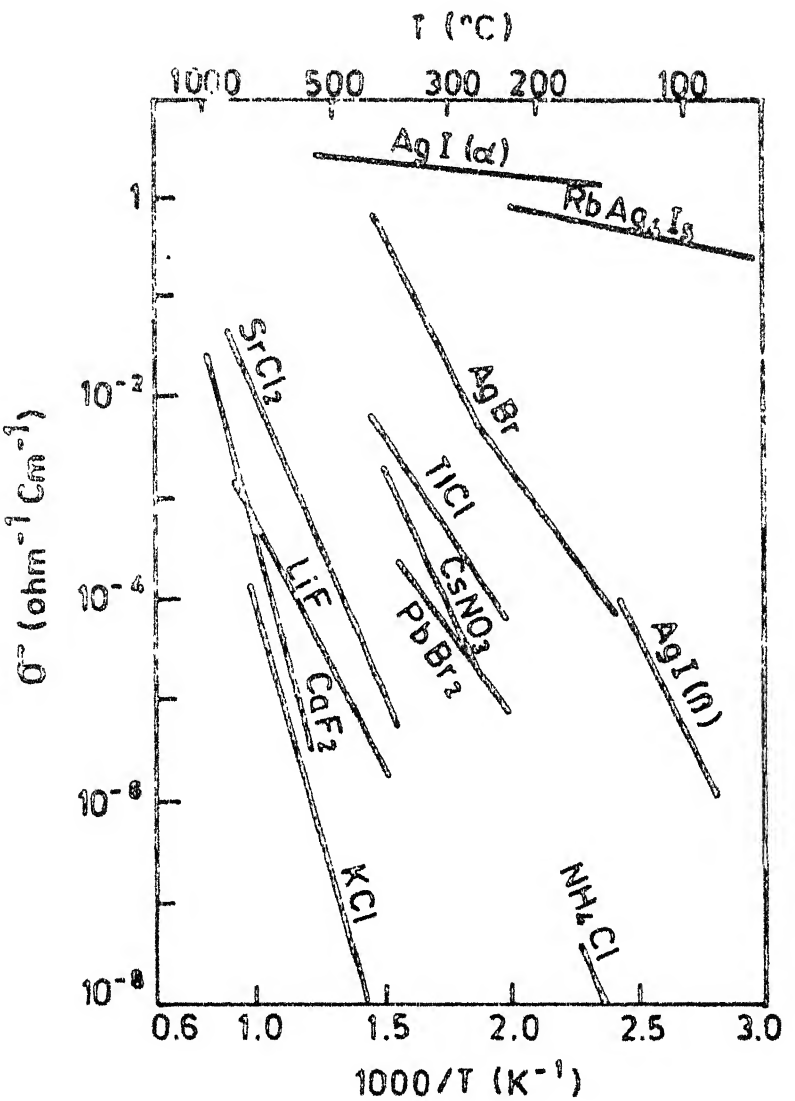

Fig. 1.1 Electrical conductivity as a function of temperature for various solid electrolytes.
(Friauf R.J. in "Physics of Electrolytes", vol 1, ed Hladik. J, 1972)

structures.

In nearly perfect crystals, ionic diffusion is always connected to the presence of lattice defects. Diffusion through vacancies and diffusion through interstitial sites are the most common types of diffusion in crystal. Such motion of ions in ionic crystals creates a net ionic current under the influence of an external field. The electrical conductivity σ is generally described by an Arhenius equation

$$\sigma = ne\mu \quad .. \quad .. \quad (1.1)$$

where n is the concentration of charge carriers, given by

$$n = A \, Exp \, (- h_f / 2kT) \quad .. \quad .. \quad (1.2)$$

and μ is the mobility of the defects given by

$$\mu = \frac{B}{T} \quad exp \, (-hm / kT) \quad .. \quad .. \quad (1.3)$$

A and B being constants, and e the electronic charge. From eqs. (1.1), (1.2) and (1.3), we get,

$$\sigma = \sigma_o \quad exp \, (\, - \frac{h_f / 2 + h_m}{kT} \,) \quad .. \quad .. \quad (1.4)$$

or $$\sigma = \sigma_o \, exp \, (- \frac{Ea}{kT}) \quad .. \quad .. \quad (1.5)$$

where $E_a = {}^1/_2 \, h_f + h_m$, h_f is called the formation enthalpy, h_m the migration enthalpy of the defects, and E_a the overall activation energy,

The pre-exponetial factor $\sigma_o = \frac{\alpha \, e^2 \, a^2 \, N \, \nu_o}{k \, T} \, exp \, (\frac{S_f / 2 + S_m}{k})$

where a is the jump distance, N the number of cation/ anion sites ν_o lattice vibrational frequency and S_f and S_m entropy of formation and migration of the defects respectively.

The above theory was essentially developed for the case of dilute point defect systems (e.g. alkali halides). Rice and Roth (1972) proposed a free-ion model for superionic conductors. This model is given below.

The superionic or fast ion conductors are different in several respects from the well known conventional ionic condctors (e.g. NaCl). Firstly, there is vast difference in the magnitude of the ionic conduction involved. It is notable that in contrast to the case of coventional ionic conductors, the large conductivities of the solid electrolytes are attained at relatively small fractions of their melting points, and with correspondingly low activation energies for ionic transport. Another major difference, connected with the high level of ionic conductivity, is the fact that the number of potentially mobile ion species, or 'carriers', in the solid electrolytes is both large and fixed, independent of the absolute temperature. In the conventional ionic conductors, the number of potential carriers is small and usually temperature dependent (Schottky or Frenkel defects are thermally activated). Another, and potentially exciting difference, is that in some of the solid electrolytes, most notably in those belonging to the oxide group, it appears possible that the mobile ionic carrier is transported in a cooperative fashion over "mean-frce paths" that are typically many interionic distances. In the conventional ionic conductors the effective ionic mean-free path for ionic charge transport is the interionic hopping distance.

The physical mechanism of ionic transport in the solid electrolytes, as in the case of the conventional ionic conductors is that of the thermal excitation of an ion from a locallized

oscillatory state to a state in which the ion moves translationally through the solid to some other available localized state situated at some finite distance from the locality of its initial state.

Arrhenius formula for the ionic conductivity given by equation (1.5) is very useful to describe the hopping mechanism of the conventional ionic conductors. Through this is qualitatively valid for many cases, it is in practice rather unsatisfactory from the point of view of obtaining relevant information from experiment . For example, although an Arrhenius formula accounts in a natural way for the exponential temperature depedence of the observed conductivity, it can not be used to deduce emperical values of say the mean hopping distance, since knowledge of the other key parameter $\bar{\nu}$, the mean local ionic oscillator frequency is quite unknown. Also, for the solid electrolytes, it is not clearly known the application of the Arrhenius theory of ionic conductivity to discribe, an a microscopic basis, the ionic transport effects such as thermoelectricity, thermal diffusion, and ionic response to a time dependent electromagnetic field.

Assume that there exists in the ionic conductor an energy gap, ϵ_o, above which ions of mass M, belonging to the conducting species, can be fhermally excited from localized ionic states to free-ion like states in which an ion propagates energy $\epsilon_m = {}^1/_2 M v_m^2$. Also assume that the energy spectrum of these elementory excitations to be continuous for all energies $\epsilon_m \geq \epsilon_o$ and to vanish for any $\epsilon_m < \epsilon_o$. Such an excited free-ion like state, on account of the interaction while the rest of the solid, is supposed to have a finite life-time τ_m .

Let $\frac{n_m}{4\pi}$ denote the probability that an ion has been thermally excited to a free-ion like state of energy $\in_m$ ($\geq \in_o$) in which it propagates through the conductor within the solid angle dV. n_m is the thermal occupations of the various free-ion like states.

Assume that the propagation velocity, v_m, and hence the energy $\in_m$, is independent of the direction of propagation. Then the total number of thermally excited free-ion like states per unit volume, N, may be written as

$$N = \frac{1}{V} \sum_m \int \frac{n_m}{4\pi} \cdot dV \qquad .. \qquad .. \qquad (1.6)$$

where V is the volume of the conductor and the sum is over all possible free-ion energy states. For sufficiently small valuesof n_m we shall assume that at a finite temperature T, the Gibbs free energy of the conductor may be expended according to

$$G = G_o + H - T \triangle S$$

$$= G_o + \sum_m \int \frac{\in_m n_m}{4\pi} dv - kT \sum_m \int \left(\frac{n_m - n_m \log n_m}{4\pi} \right) dV.$$

where G_o is a constant independent of n_m the equilibrium thermal occupation is

$$n_m^o = e^{-\in_m / kT} \qquad .. \qquad (1.8)$$

Replacing the summation over m with an integral as

$$\frac{1}{V} \sum_m \rightarrow \int_o^\infty f(\in_m) \, d\in_m \qquad .. \qquad .. \qquad (1.9)$$

$f(\in_m)$ is the density of states function. Then equation (1.6) becomes

$$N = \int_0^\infty d\epsilon_m \cdot f(\epsilon_m) \int \frac{n_m}{4\pi} \, dV \quad .. \qquad (1.10)$$

Since ϵ_m has been assumed to be independent of direction $v_m/|v_m|$, we have at equilibrium,

$$N_o = \int_0^\infty d\epsilon_m \cdot f(\epsilon_m) \; e^{-\epsilon_m / kT} \quad .. \qquad (1.11)$$

Since it is essumed that the free-ion like states originate from the thermal excitation of ions of the conducting species from their localized states in the conductor,

$$\left.\begin{aligned} f(\epsilon_m) &= 0 \qquad \text{for } \epsilon_m < \epsilon_o \\ \text{and} \qquad f(\epsilon_m) &= n/kT \quad \text{for } \epsilon_m \geq \epsilon_o \end{aligned}\right\} \qquad (1.12)$$

substituting (1.12) into (1.11), the total number of free-ion like states thermally excited per unit volume at equilibrium is

$$N_o = n e^{-\epsilon_o / kT} \quad .. \qquad (1.13)$$

Let $n_m(r,t)$ denote the value of the thermal occupation of the free-ion like state of energy ϵ_m at time t in the vicinity of a point r within the conductor. The ionic current at the point (r, t) will be given by

$$i(r, t) = q \int_0^\infty d\epsilon_m \cdot f(\epsilon_m) \int \frac{v_m \cdot n_m(r, t)}{4\pi} \, dV \quad .. \qquad (1.14)$$

where q is the charge carried by an ion belonging to the conducting species.

The total heat flux J is given by

$$J = -K_L \, \delta T + J_H$$

where K_L is the lattice contribution to the total thermal conductivity. δT is the uniform temperature gradient

J_H is the heat or enthalpy, current produced by the free-ion like states and is given by J_H (r, t) =

$$\int_0^\infty d\epsilon_m . f(\epsilon_m) \int \frac{\epsilon_m v_m n_m (r, t)}{4\pi} dV \quad .. \qquad (1.15)$$

In the absence of an electronic component of transport, the ionic current is

$$i = \sigma E$$

where E = electric field

The ionic conductivity is given by

$$\sigma = \frac{q^2}{kT} \int_0^\infty d\epsilon_m \, f(\epsilon_m) \int \frac{n_m^o \tau_m v_m^2}{4\pi} dV \; . \quad (1.16)$$

where n_m^o is the equilibrium thermal occupation. Under isotropic conditions, the ionic conductivity is given by

$$\sigma = \frac{1}{3} \left(\frac{q^2}{kT}\right) n v_o l_o e^{-\epsilon_o / kT} \quad .. \qquad (1.17)$$

where l_o = mean-free path of the free-ion like state excited at the gap energy $\epsilon_o = v_o \tau_o$

and v_o = velocity = $\sqrt{2\epsilon o/M}$

τ_o = life time of the free-ion like state.

The Arrhenius expression for the ionic conductivity resulting from the concentration $n_i(T)$ of interstitial ions at σ temperature T, assuming cubic symmetry is

$$\sigma = \frac{1}{3} \left(\frac{q^2}{kT}\right) n_i (T) \; a^2 \nu \; e^{-E/kT} \quad .. \quad (1.18)$$

Here 'a' denotes the hopping distance between an interstitial ion and a neighbouring (vacant) interstitial site.

ν the vibrational frequency of the localized interstitial ion and E the migration energy required to effect the ionic hop. q is the charge on the interstitial. Comparing (1.18) with (1.17) and identifying $n_i(T)$ with n and E with ϵ_o, the two expressions differ only in the factor $v_o l_o$ appears in (1.17) in place of the product $a^2 \nu$ that appears in (1.18).

ν in the coventional hopping theory is in fact equal to the inverse of τ_o. Thus, for the interstitial mechanism (1.17 and (1.18) are equivalent.

It is to be noted that both equations (1.17) and (1.18) assume a simple form of the type

$$\sigma T = A \exp (- E_a / kT) \qquad (1.19)$$

where A is a constant. Thus a plot of $l_n (\sigma T)$ versus $1/T$ should be a straight line of slope equal to $-E_a / k$. It should be pointed out that since the variation of $l_n T$ is often negligible compared to variation of $l_n \sigma$, the $l_n \sigma$ versus $1/T$ plot is also found to be linear within the exponential error, and is more often used to express the experimental data. The additional advantage of such a plot is that the conductivity values at various temperatures can be easily obtained directly from the plot.

1.1.3 General Applications of solid electrolytes

Common solid electrolytes are basically of three kinds: simple or complex halides, simple or complex oxides , or oxide-solid solutions. Of these, the oxide-solid solutions (e.g. ZrO_2-CaO, ThO_2-Y_2O_3) are by far the most commonly used in solid electrolyte work, followed by complex oxides such as β - alumina and complex halides (e.g. Rb Ag_4I_5). Commercial

applications of solid electrolytes also are so far, restricted mostly to these.

The three fundamental principles governing the practical applications of a solid electrolyte are : (1) the material provides an impervious barrier to gases and liquids. The material, however, allows one or more kinds of ions to migrate through its lattice when a tendency for such migration exists. (2) A solid electrolyte allows the measurement of the difference of chemical potentials of the migrating species on either side of it in terms of electromotive force in a properly constiuted cell. (3) solid electrolytes are stable compounds not easily corroded by high temperature environment.

The main applications of solid electrolytes fall into the following categories :

(a) closed-circuit applications : Here the solid electrolyte under induced external voltage is a medium of mass transfer.

(b) open-circuit applications : In these applications the solid electrolyte is employed in suitable e.m.f. cells which serve, e.g. as meters for exygen in metals or gases.

(c) energy conversion : Here the solid electrolyte provides the electrolytic medium necessary both for ionic migration as well as development of electromotive force.

(d) solid state batteries : In these ionic transport of solid electrolytes is utilized for energy storage.

(e) solid state ionics : Here ionic conductivity of solids is used in a range of devices such as energy conversic devices, capacitors, timers, coulometers , transducers, etc.

The two main principles governing the closed-circuit appli cations are (a) The e.m.f. of a solid electrolyte galvanic cell gives thermodynamic information concerning chemical potentials or activities at the electrodes provided conduction is completely ioni (b) The current through a cell such as

$$pO_2,\ Pt/ZrO_2 + CaO\ \ Pt,\ pO_2$$

is a measure of the rate at which oxygen is passed from one side of the cell to the other. Since only oxygen ions can pass through the electrolyte when the electrical circuit through the electron-conducting leads is closed, it follows that oxygen transfer across the solid electrolyte may be controlled by controlling the current provided the current does not exceed the limiting current for transport processes.

While the first principle is useful from the view point of fundamental studies regarding kinetics of certain reations, from the second principle it is evident that the solid-electrolyte cell is very useful as a device for controlled oxygen trnasfer to and from gaseous or liquid metallic media.

An example for the open-circuit applications is the solid electrolyte cell as oxygen meter useful for the measurement of oxygen concentration in gases and determination of oxygen in liquid metals and alloys.

In various reactions, the concentration of oxygen in various phases is an important parameter which often needs to be measured, monitored, and controlled. Over the years, various techniques such as spectrometry, gas chromatography, redox titration, polarography, electrode potential measurement, solid-electrode voltametry, fluometric methods, etc. have been employed for oxygen analysis. But the discovery of the oxygen-ion-conducting solid electrolyte and the ability of an electrochemical cell based on it to measure oxygen potential has led to a breakthrough in the field of continuous oxygen concentration measurement. Some of the advantages of these solid-electrolyte oxygen sensors are

a) E.M.F. response of the cell is usually specific, rapid and continuous.

b) A single sensor can often cover exceedingly wide range of oxygen potential and temperature.

c) E.M.F. measurement can be made directly on the system to be investigated.

d) Since the output voltage can be amenable to fast and continuous measurement, the meter is ideally suited as a transducer for recording and feed back control.

e) It is versatile and since it measures oxygen potential specifically, it is applicable for oxygen analysis in any material.

These sensors have some inherent limitations also. For example, the device using ZrO_2-CaO or ThO_2-Y_2O_3 can not be used below 500°C or so because of high resistence and irreversibility. Secondly, oxide solid electrolytes have very poor thermal shock resistence and great care is needed in order to prevent thermal cracking.

The devices employed in direct energy conversion can be classified under electrochemical, thermoelectric, thermoionic, photovoltaic, and magnetohydrodynamic methods. Solid oxide electro lytes have found use in electrochemical, thermoelectric, and magnetolydrohynamic generators. Of these, all the methods other than photovoltaic energy converters are limited by the Carnnot efficiency. On the other hand, since a fuel cell works isothermall its efficiency bears no relationship to the Carnnot efficiency.

The fuel cell is a primary electrochemical device where a fuel is fed to one electrode (anode) and oxidant to the other electrode (cathode). Generally the oxidant is oxygen or air. The chemical energy derived from the oxidation of fuel is continuously converted to electrical energy. The fuel and the oxida are separated by an electrolyte, which is predominantly oxygen ion conducting in the case of a solid oxide electrolyte fuel cell. The differencein the chemical potentials between the two electrodes manifests itself in the form of an electromotive force. When the electrodes are connected through a load, a current passes in the external circuit and the fuel gets oxidzed.

When a voltage is applied across the interface of an electronic and ionic conductors, charges accumulate as in the charging of a capacitor whose plates are separated by distances of only atomic dimensions. As a result of this small distances, remarkably high capacitances can be achieved in small volumes.

An electrode which permits a flow of ions, e.g. silver in the case of Ag^+ -ion-conducting electrolytes, together with a blocking electrode can be used to make a timing device.

Solid electrolytes have a vast potential for use in sensing devices. A silver-ion-conducting electrolyte can be used in temperature and pressure-sensing elements by using two silver electrodes across a thin pellet of the electrolyte. Strain gages employing solid electrolytes can be used for long-term monitoring of deformable elements in inaccessable places and do not need any axsiliary power supply. Calcia-stabilized zirconia is useful as heating elements and as electrodes in magneto hydrodynamic generators.

1.2 ROLE OF Li AND Na ION CONDUCTORS

Over the last few years there has been rapidly accelerating interest in solid electrolytes because of the interesting scientific problems which they pose, and because of their application in a number of important technological devices. Several solid electrolytes have been used for a variety of technical applications, such as oxygen gas sensors, timers, coulometers and ion-selective electrodes. A large scale application of the solid electrolyte is the separator in batteries. One of the most important and widely used solid electrolyte material in this field was the β - alumina. The β -alumina family represents a group of materials with very high conductivity for sodium ions. The two most important members of the family are the hexagonal form (designated β) and the rhombohedral form(designated β'') . The formula of β -alumina derived from the crystal structure is $Na_2O.\ 11\ Al_2O_3$ but it always contains excess soda. The forula of β''-alumina is $Na_2O.5\ Al_2O_3$ but it is soda deficient and is normally stabilized by the addition of MgO and/or Li_2O.

Table 1.2 gives ionic conductivity of various sodium ion conductors at room temperature.

Table 1.2

Material	Conductivity at 25°C (ohm. cm)$^{-1}$
Sodium β-alumina	1.4×10^{-2}
Sodium β-Gallate	3×10^{-3}
$Na_3 ZrSi_2PO_{12}$	2×10^{-4}
$Na_5 YSi_4 O_{12}$	5×10^{-4}
Polyether complexes	10^{-6}

Fig. 1.2 shows the variation of conductivity with temperature for various sodium ion conductors.

The main application of the β-alumina is in the sodium-sulphur battery. The sodium-sulphur system when fully engineered will be capable of giving a specific energy of 762 Wh/Kg. Practical energy densities of the order of 330Wh/Kg. have already been achieved compared to a value of 30-40 Wh/Kg. for the common lead-acid battery. The Na/S cells are capable of yielding very high current densities $\sim$ 400mA/cm^2. The batteries can be reacharged at a high efficiency even at very high charging rates.

The other applications of β-alumina are in primary cells using sodium-mercury amalgam as the anode and water, air,or halogens as the cathode. The cells operate around the ambient temperatures and have been proved to give high cell voltage and energy densities. Iron doped sodium β

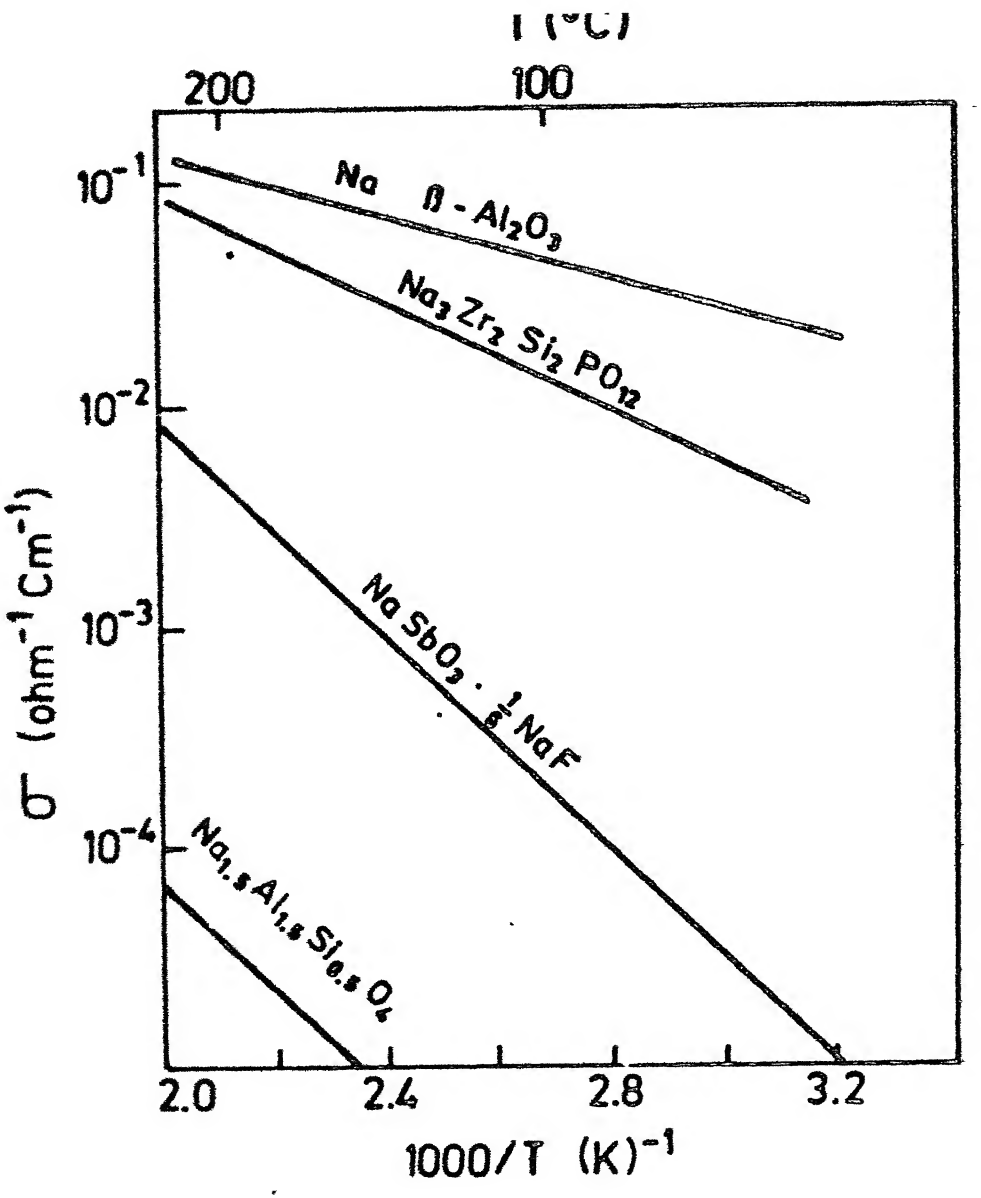

Fig. 1.2 Electrical conductivity as a function of temperature for various sodium ion conductors.

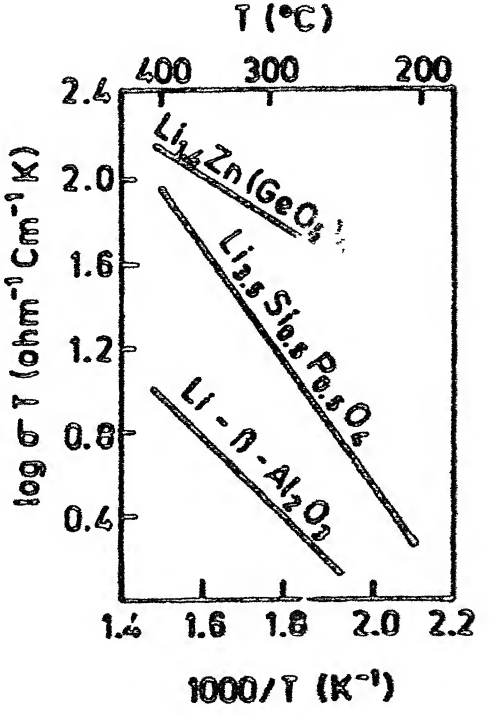

Fig. 1.3 Electrical conductivity variatio of various Lithium ion conduc ors with temperature.

be used as cathodes in galvanic cells based on β-alumina. β-alumina has a protential for direct energy conversion in a hybrid system coupled to a sodium-cooled nuclear reactor.

Lithium ion conducting solid electrolyte batteries have been developed and successfully applied to applications requiring high energy density. The development of these primary batteries was concurrent with the advanced development of cardiac pacemakers, which had a need for very low power batteries capable of long life operation. The convergence of these two technologies during the past decade has been largely responsible for the development of the present commercially available lithium solid electrolyte batteries.

Lithium based electrochemical cells became popular because of the low equivalent weight of Li metal and its high electropositivity which give rise to high cell voltages and energy densities. Li metal is not expensive and can be much more easily handled at room temperature than the other alkali metals. Furthermore several cathode materials are known which might be employed in lithium transporting systems because of their relatively high lithium diffusion coefficients.

The three main requirements for solid Li-electrolytes are high Li ion conductivity of at least 1×10^{-3} ohm^{-1} cm^{-1} at the operation temperature of the cell combined with a negligible partial electronic conductivity, stability of the electrolyte with electrodes of high Li activities and the production of a suitable polycrystalline sinter, which is cheap and easy to fabricate.

Table 1.3 gives the room temperature conductivities for various Li ion conductors.

Table 1.3

Ionic conductivity of some selected Li^+ based fast ion conductors

Material	Conductivity at 25°C $(\text{ohm}\cdot\text{cm})^{-1}$
Li_3N	10^{-3}
Li/ Na-β- alumina	5×10^{-3}
$LiX.H_2O.Al_2O_3$ ($X = I^-, Br^-, Cl^-, F^-$)	$10^{-5} - 10^{-2}$
$LiX.H_2O.SiO_2$	$10^{-5} - 10^{-3}$
$Li_{14}Zn(GeO_4)_4$	$< 10^{-5}$
$LiI.Al_2O_3$	10^{-5}
Polyether Complexes	10^{-6}
LiI	$1.2\text{-}4.9 \times 10^{-7}$

Fig. 1.3 shows the temperature variation of electrical conductivity for various Li ion conductors.

1.3. ADVANCED SOLID ELECTROLYTE BATTERIES

The prevalent energy crisis and the rapidly multiplying ecological problems brought about a search for energy sources based on renewable, nonfossil fuels. Widespread resurgence of interest in rechargeable cells has resulted in the development of a number of high-energy battery systems using solid electrolytes.

An ideal solid electrolyte to be employed in a cell or battery must possess the following properties.

(1) The electrolyte (or ionic) conductivity of the solid electrolyte should be as high as possible. Otherwise the voltage drop across the internal resistence of the cell lowers the operating voltage of the cell significantly. Further, the temperature dependence of conductivity, (i.e. the activation energy) of the solid electrolyte should be low so that the performance of the cell does not vary much with the temperature.

(2) The electronic conductivity of the electrolyte should be as low as possible, otherwise it lowers the shelf life of the cell.

(3) The solid electrolyte should be compatible with the electrode systems. Also the solid electrolyte should be fairly stable under ambient condictions such as ambient temperature, pressure, humidity and atmosphere.

(4) Ionic transference number of the solid electrolyte should be approximately unity.

(5) Decomposition potential of the solid electrolyte should be high.

Table 1.4 gives the performance characteristics of various energy storage batteries.

The characteristics of some of the solid electrolyte battery systems operable at room temperature and employing pure metallic lithium as the anode are given in Table 1.5.

Performance figures of various energy storage batteries

Batteries	Typical temperature (°C)	Conductivity of the electrolyte $(ohm.cm)^{-1}$	Battery voltage at discharge (V)	Current density (A/cm^2)	Specific power (W/Kg.)	Specific energy (Wh/Kg.)	Shelf life (cycles)
Led-acid	40-50	6.536×10^{-1}	2.1-1.46	0.01	7-30	~ 40	10-400
Nickel-iron	0-40	5.1×10^{-1}	1.3-0.75	-	7-40	30-35	100-3000
Nickel-cadmium	40-60	5.1×10^{-1}	1.3-0.75	0.01	7-44	35-40	100-2000
Silver-zinc	0-40	5.1×10^{-1}	1.55-1.1	0.45	24-150	80-100	100-300
Silver-cadmium	40-60	5.1×10^{-1}	1.3-0.8	-	20-66	50-60	500-1100
Lithium-chlorine	650	5.88	3.40	1-3	80-150	330	-
Sodium-sulphur	300	0.2	2.08-1.76	0.7	330	330	2000
Sodium-air	130	2.793×10^{-1}	2.3	0.07	90	350	-
Zinc-air	25	-	1.4	-	60	200-300	300-400
Lithium-tellurium	450-480	3.846	1.79-1.67	2-5	280	180	-
Sodium-bismuth	540-580	2.273	0.8-0.44	0.5-1	80	40	500

Table 1.5

OCV and energy density of various Li-batteries (after Shahi et.al) 1983

Battery configuration	Open circuit voltage (V)	Energy density (Wh cm^{-3})
Li ‖ LiI ‖ AgI, Ag	2.10	
Li ‖ LiI ‖ I_2 (Org)	2.80	0.4-1
Li ‖ LiI (Al_2O_3) ‖ CuI, Cu	2.08	
Li ‖ LiI (Al_2O_3) ‖ AgI, Ag	2.11	
Li ‖ LiBr ‖ Br_2, PVP	3.50	~1.25
Li ‖ Li_3N-LiI-LiOH ‖ Pb-I_2,PbS	1.90	~ 0.5

1.3.1 Present status and the statement of the problem

Realizing the importance of energy storage systems, various test cells have been developed using appropriate anodes (mostly pure elements) and a variety of cathodes, and their performance examined under varying conductions. But for high energy density the requirement of highly conducting electrolyte and the corresponding highly electropositive metal anode have led to the realization of the vast potential of alkalimetals as anodes, in particular lithium, and hence Li^+- based solid electrolytes. A wide variety of solid electrolyte based on Ag^+ and Cu^+ ion transport have been extensively used in development of cells but failed to reach the commercial stage.

There are a number of Li^+ based solid electrolyte available (Table 1.3, Fig. 1.3). However most of these seem to suffer from certain disadvantages. For example, Li_3N, one of the best Li^+ ion conductor, is not stable in air and also has very low

decomposition potential. Similarly Li-β- Al_2O_3, another important Li^+-based Fast ion conductors, is apparently unstable in contact with solid Li anode. Thus there is a genuine need for the development of new and better Li^+-based solid electrolytes which could meet most of the requirements for battery applications.

We have studied Li_2SO_4-based solid electrolytes. Li_2SO_4 was chosen because it is one of the best Fast ion conductors, however at T $\geq$ 575°C. The present work was aimed at lowering the superionic transition temperature, and theseby stabilizing the superionic α -Li_2SO_4 phase near room temperature. LiCl has been explored as a stabiliging agent.

In contrast to the anode, numerous posibilities exist for the selection of cathode. The direct use of elemental oxygen or the chalcogens (S, Se, Te) as the cathode is not practical. However, salt complexes of certain halogens plus excess iodine or bromine, or polyiodides (e.g. $Me_4 NI_n$, n = 3,5,9) have been very useful. A third group consists of metal salts such as PbI_2, PbS, $As_2 S_3$ and TiS_2. Practical cathode have been found in both of the latter two groups. Some metal oxides such as PbO_2, MnO_2, Ag_2O, CuO and Bi_2O_3 are seen to be promising cathode materials, but have not been tried in solid electrolyte lithium batteries.

Table 1.6 gives the performance characteristics of some commercial solid electrolyte lithium batteries.

Table 1.6

Performance characteristics of some commercial solid electrolyte lithium batteries.

Battery configuration Battery configuration	Open ckt. voltage (V)	Energy density (Wh/cm^3)	Manufacturer/ reference
Li ‖ LiI ‖ I_2, PVP[a]	2.80	~1.0	CRC[b], WGL[c]/ Great batch et.al (1971)
Li ‖ LiI(Al_2O_3) ‖ PbI_2, Pb	1.91	~0.2	DC[d]/ Liang (1973)
Li ‖ LiI(Al_2O_3) ‖ PbI_2, Pbs, Pb	1.91	~0.6	DC[d]/ Liang and Barnett (1976)

[a]PVP = Poly (2-Vinylpyridine), reacted with I_2 at either elevated or ambient trmperature.

[b]CRC = Catalyst Research Corporation, 1421 Clarkview Road, Baltimore, MD 21209, USA.

[c]WGL = Wilson Greatbatch Ltd., 4098 Barton Road, Clarence, NY 14031, USA.

[d]DC = Duracell Internationa Inc., Northwest Industrial Park, Burlingron, MA 01803, USA.

The battery systems which are commercially available are characterized by long shelf life, low rate, high energy density (0.2-1 Wh/cm^3) and high reliability. All involve low vapour pressure components and can thus be hermetically sealed. They have proven their capability for long term implantable biomedical applications and are finding application in memory and watch batteries in electronic devices.

2. EXPERIMENTAL TECHNIQUES

2.1 INTRODUCTION

Solid electrolytes are presently of particular interest for various practical applications such as high energy and power density batteries, fuel cells, electrochromic desplays, sensors, etc. Lithium ion conductors are of predominant importance due to the low atomic weight and more electropositivity of lithium element. Furthermore, many of the lithium and sodium compounds have high Gibbs free energies of formation, which essentially means a large open circuit voltage (OCV) and hence large energy density for lithium batteries. These advantages have led to the search for new and better fast ion conductors based on Li^+ or Na^+ ion transport. And in fact as a result of this, several good Li^+ and Na^+ ion conductors have already been discovered (eg. Li-β-Al_2O_3, Li_3N, Na-β-Al_2O_3, Na-β''- Al_2O_3, etc.), but they all seem to have some problems regarding stability either in atmospheric conditions or in battery conditions, which limits their applications. Thus, there is genuine need for new better and stable solid electrolytes based on Li or Na.

The sulphate based solid electrolytes differ from other solid electrolyte materials in the sense that they allow rapid transport of not only monovalent Li^+ ion but also several divalent cations eg. Mg^{2+}, Ca^{2+}, Zn^{2+}. The conductivity phases develop through first-order phase transitions with exceptionally high enthalpies of transformation also makes these materials interesting for heat storage.

There are two crystalline modifications of lithium sulphate, the low temperature modification β-Li_2SO_4 ($T \leq 575°C$) and the high temperature modification α-Li_2SO_4 ($T > 575°C$). The electrical conductivity of α-Li_2SO_4 has been measured over the temperature range 575-970°C (Kvist, 1965), Benerath and Drekopf (1921) have studied the f.c.c. phase of Li_2SO_4 in great detail . Since this high conductivity (fast ion) phase is stable only above 575°C, its use in practical devices is rather limited. It was therefore felt necessary to increase the conductivity by some treatment to a value suitable for power sources. Kvist et.al. (1966,1969,1970) have studied the conductivity of binary systems of Li_2SO_4 over the temperature range 500-1030°C. Friauf (1976) has shown that all observations involving conductivity and diffusion in the region just below the melting point may be explained as being due to an anomalous rise in the defect concentration caused by a general softening of the lattice.

The present investigation, taking all the above facts into account, is aimed at developing a lithium sulphate-based material that gives high ionic conductivity at relatively lower temperatures. With this in view, the eletrical conductivity of the Li_2SO_4-LiCl system has been studied over the range 10-90 mole % Li

2.2 . STARTING MATERIALS

Starting materials needed for the present study are Li_2SO_4 and LiCl. Hydrous lithium sulphate, i.e. $Li_2SO_4H_2O$ was obtained from Indian Drugs and Pharmaceuticals Ltd. (India) and LiCl from SISCO (India).

Tables 2.1 and 2.2 give the chemical analysis of $Li_2SO_4H_2O$ and LiCl respectively as provided by the suppliers.

Table 2.3 gives the characteristics of Li_2SO_4 and LiCl.

Table 2.1

Chemical analysis of $Li_2SO_4H_2O$

Mol. Wt. = 127.95	
Assay (Minimum)	98%
Impurities (maximum)	
Chloride	0.01 %
Nitrate	0.01 %
Iron	0.002 %
Lead	0.003 %

2.3 PREPARATION OF PELLETS

Pellets of pure Li_2SO_4 and pure LiCl were prepared in two ways. In the first case, the materials were dried before using and in the second case they were melted before pelletization. This was thought desirable to see the effect of thermal history, etc.

$Li_2SO_4H_2O$ was heated to about 150°C in an oven for ~5 hrs to remove the water content. The dried powder was finely ground for about 20-30 minutes in a pestle and mortar.

Table 2.2

Chemical Analysis of LiCl

Mol. Wt. = 42.59	
Assay (minimum)	99%
Impurities (maximum)	
Sulphate	0.005%
Arsenic	0.00005%
Iron	0.0005%
Heavy metals (Pb)	0.0005%
Total nitrogen	0.001 %
Calcium	0.005%
Magnesium	0.005%
Barium	0.005%
Sodium	0.05 %
Potassium	0.05%

Extra pure LiCl was heated to about 120°C for ~5 hrs. to remove any moisture present in the material. The dried powder was then finely ground and pellets were made as described below.

For the pre-melted materials preparation, monchydrate lithium sulphate ($Li_2SO_4H_2O$) was taken in a porcelain crucible, heated to about 150°C for ~4 hrs. in a box-type induction furnace. The temperature was then raised to its melting point (860°C), let it stand there for 10 minutes, followed by air quenching by way of transferring the melt onto a clean aluminium

Table 2.3

Characteristics of Li_2SO_4 and LiCl

Material	Melting Point (°C)	Crystal Structure	Lattice Constant[+] (A°)	Reference
Li_2SO_4	860	Monoclinic (β-Li_2SO_4, stable at $T \leq 575°C$)	a = 8.241 b = 4.953 c = 8.474 β = 107°58.8'	Swanson et.al (1968)
		f.c.c. (α -Li_2SO_4, stable at $T > 575°C$)	a = 7.07 (at 610°C)	Forland and Krogh-Moe (1957)
LiCl	606	Rocksalt	a = 5.129	Wyckoff (1963)

[+]The lattice constants are at room temperature unless otherwise specified.

sheet. The fact that the porcelain crucible does not give any contamination to Li_2SO_4 was confirmed by Deshpande and Singh (1982). We also did not notice any apparent contamination so as to produce a clear change or decomposition, etc. No other tests for contamination were done, nor was felt desirable. The resolidified Li_2SO_4 was then finely ground and used for making pellets.

LiCl was also first heated in a porcelain crucible to about 150°C for ~ 4hrs. and then the temperature was raised to its melting point (606°C). The fine powder prepared in the same way as of premelted Li_2SO_4 was used for making pellets.

The compositions of 90:10, 80:20, 70:30, 60:40, 50:50, 40:60, 30:70, 20:80, 10:90 mole% of Li_2SO_4: LiCl were weighed using a digital electronic balance (Sartorius, Model No. 2006 MP) to an accuracy of 0.0001 g. Each composition was mixed and ground in an agate mortar and pestle, transferred to a porcelain crucible, heated to melting, followed by air quenching in a manner described earlier. The fine powder was used for making pellets as described below.

The fine powder so obtained above was transferred into a stainless-steel die (shown in fig. 2.1). The powder was then levelled off by means of the die-piston, the total assembly put in a hand operated, laboratory size hydraulic press, and a pressure of the order of 5 ton/cm^2 was applied. The pellets obtained in this manner were like tablets of diameter 0.976 cm, the piston diameter. The thickness of the pellets was usually in the range of 2-4 mm. The steel die was thoroughly cleaned with acetone every time before and after use.

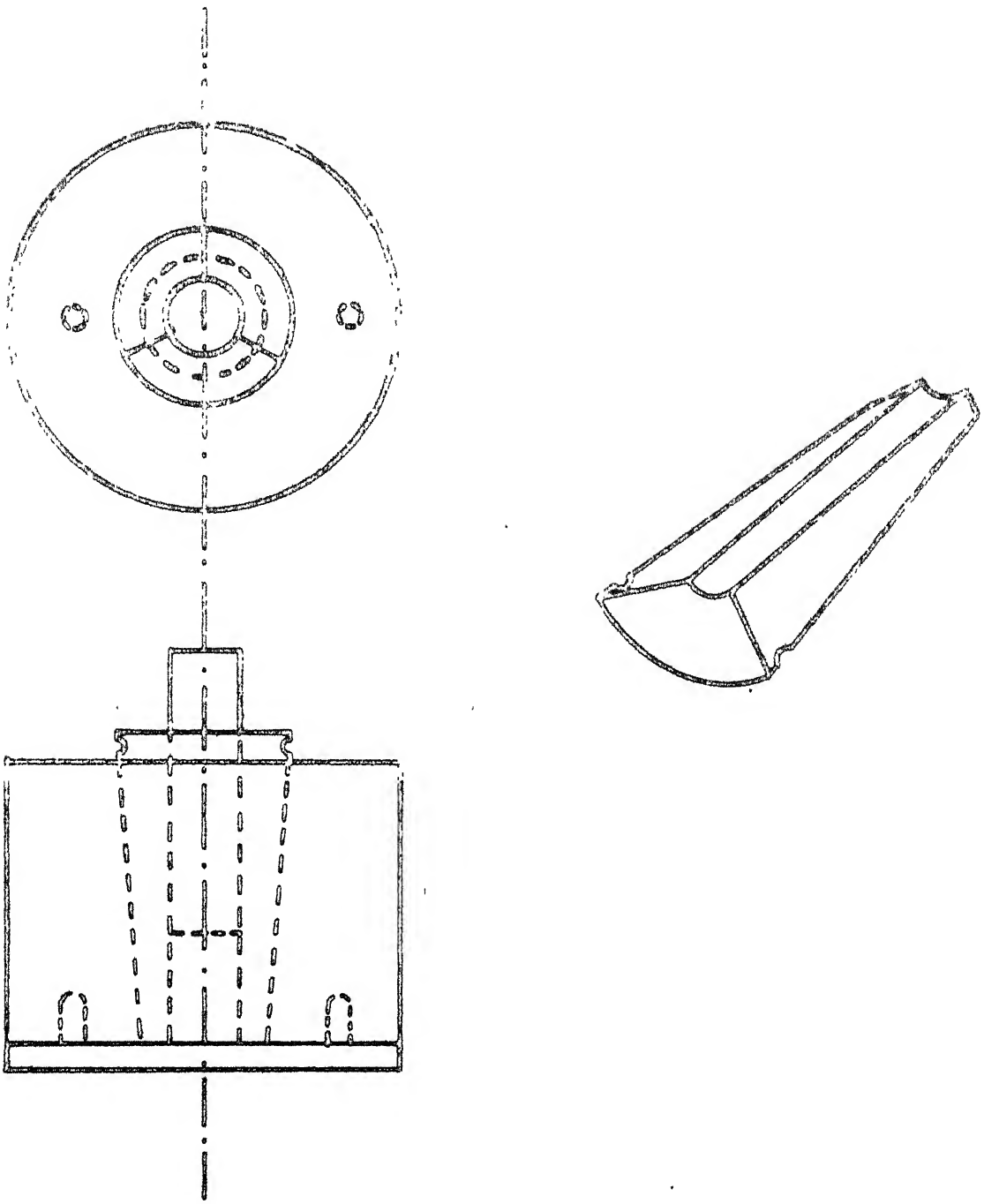

Fig. 2.1 Stainless-steel die for making pellets.

To prevent absorption of moisture the materials and pellets were stored in a desiccator throughout the duration of the work. However, since materials handling, pellet preparation, loading of the sample in the sample holder, etc. have to be done in open atmosphere, presence of some water vapour can not be ruled out at this stage. In order to minimize/ eliminate this water content, the samples were usually heated/ annealed at about 400°C for several hours before starting any measurements.

2.4 MEASUREMENT TECHNIQUES

The pellets prepared as above were polished on a clean white paper to achieve flat surfaces. The thickness of each of the polished pellets was measured using a vernier caliperse. The pellet was then loaded into a sample holder, the design of which is shown in fig. 2.2. The various components of the sample holder can be identified from the figure. Instead of backelite, tefflon or ebonite block can also be used. The lava disc has the advantage that it can be easily machined to give desired shape, size and geometry, followed by heat treatment at a high temperature (~1000°C). Once the lava disc is heat-treated, it become hard, highly insulating and then it can not be machined. The sample holder is simple, versatile and easy to handle. It can be used over a wide temperature range, from liquid nitrogen temperature to about 900°C.

For accurate measurement of electrical conductivity good contact between the electrodes and the solid is of prime importance. The present sample holder was provided with two

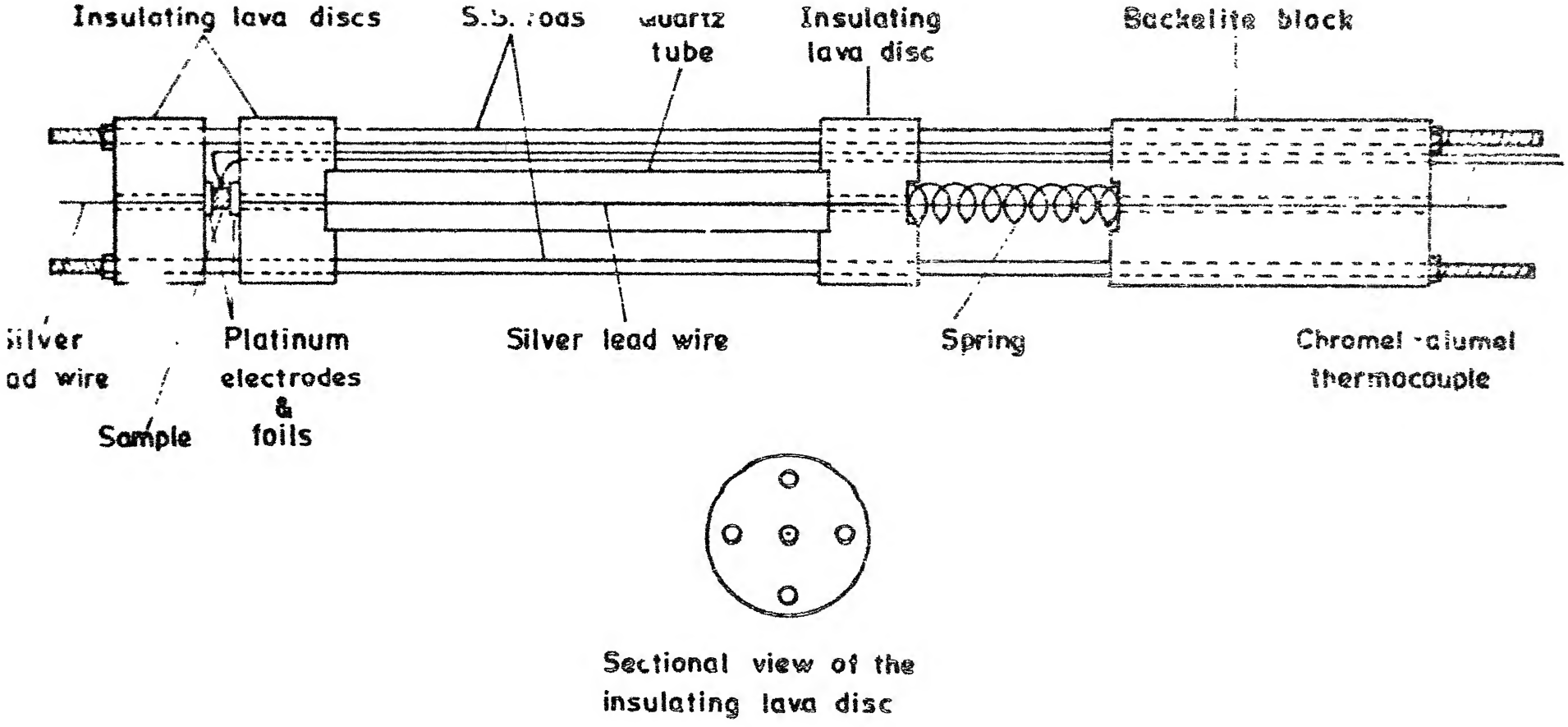

Fig. 2.2 Sample holder for the electrical conductivity measurements.

thick platinum discs of diameter nearly the same as that of pellet to serve as support electrodes. In addition to this, two thin platinum foils were inserted in between the pellet and the two thick-platinum (support) electrodes. The platinum foils are expected to provide good ohmic contact and also they can be thoroughly cleaned after each experiment, and used again.

The sample holder loaded with the sample was then kept in the furnace. Because the materials to be studied were somewhat hygroscopic the furnace was preheated to about 120°C to minimize the water absorption by the sample. The furnace which was fabricated and ensembled in our department's machine shop has a uniform winding (10 torns/inch) of Kanthal wire (20 SWG) over a mullite tube. It was closed at one end by a ceramic brick to prevent air circulation through the furnace so that the steady state is reached faster and better. The other open end was used to insert the sample holder into the furnace.

The electrical conductivity of each of the samples was measured at various temperatures during the cooling cycle. The block-diagram connections for the conductivity measurement are shown in fig. 2.3. The silver lead wires from the electrodes were connected to the 'High' and 'Low' terminals of the impedence bridge (General radio, Model No. 1608-A). Chromel-alumel thermocouple was used for temperature measurement of the sample. In order to measure the sample temperature accurately, the tip of the thermocouple was placed as close to the sample as possible.

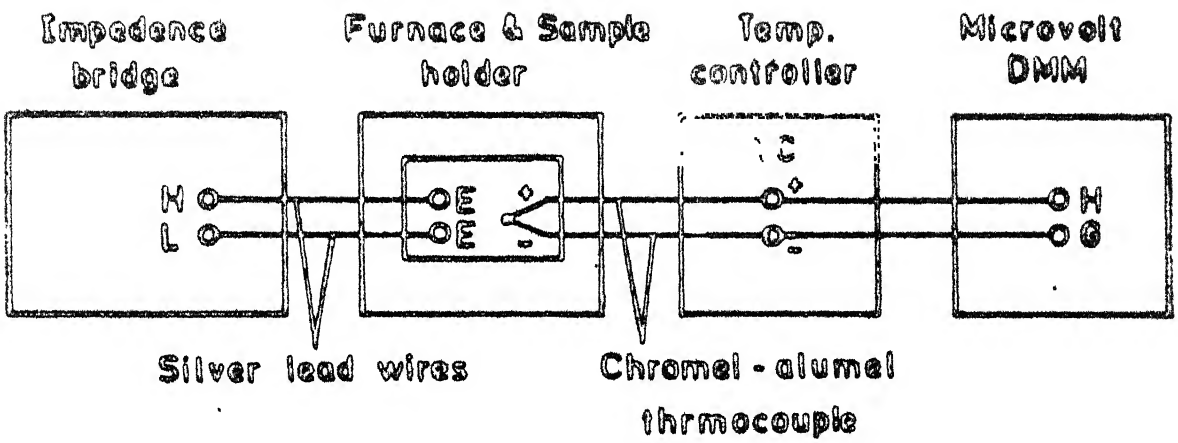

Fig. 2.3 Block-diagram connections for electrical conductivity measurements.

The free ends of the thermocouple were connected to the 'High' and 'Ground' terminals (H and G in the figure no. 2.3) of the digital multimeter (Keithley Type 177) via a temperature controller (Eurotherm). After the set temperature was reached, about 20 minutes was allowed for the sample to equilibrate at that temperature. Then the conductance value (Gp) was measured. The conductivity σ was then calculated using the simple formula.

$$\sigma = Gp. \frac{t}{A}$$

where t is the thickness of the sample and A is the contact area of the sample with the electrode. In the present study, A was fixed at 0.748 cm^2 which is same as the area of piston cross-section.

The values of log σ (ohm.cm)$^{-1}$ were plotted against 1000/T (K)$^{-1}$ for different samples. Experiments were repeated to check the reproducability of conductivity values for different samples. In general, it was observed that the conductivity measurements were more acurate and reproducible ($\pm$ 10%) at higher temperatures. However, at lower temperature the reproducability was rather poor, and also varied significantly from sample to sample. This is possible due to the fact that at lower temperatures the conductances are lower, and the resolution of the impedence bridge used for conductance measurements in these ranges is not as good. The second cause of poor reproducibility at lower temperatures may be the fact that in this temperature range the effects of grain boundaries, impurities, thermal history. etc. are much more pronounced than at higher temperatures. As such it is rather difficult to claim a uniform reproducibility figure for all the samples. However, we do

wish to mention that for the majority of the samples, reproducibility in the low temperature range was better than $\pm$ 40%. This can be improved upon by making use of external generator (e.g. GR 1310) and amplifier-detector (GR-1232 PZ) which provides much better resolution than the built-in null detector of GR 1608A impedence bridge. Unfortunately we do not have the former two pieces of equipments.

3. RESULTS AND DISCUSSION

3.1 STARTING MATERIALS

3.1.1 Lithium Sulphate

Lithium sulphate has two solid phases; The high-temperature phase, designated as α-Li_2SO_4, is stable between 575°C and the melting point (860°C), and the low-temperature phase called β-Li_2SO_4 is stable below 575°C. The high-temperature α-phase has a face centered cubic (f.c.c.) structure with a = 7.07Å at 610°C in which the number of available cation sites is 50% larger than the number of lithium ions to occupy them (Forland and Krogh-Moe, 1957). This type of massively defective structure is termed as 'average structure" and is a common feature of all fast ion conductors. This structural disorder is highest for α-AgI in which there are 12 cation sites and only 2 Ag^+ ions per unit cell, and as a result α-AgI exhibits the highest conductivity of $\sim$1 $ohm^{-1} cm^{-1}$ at 150°C. The high temperature α-phase of Li_2SO_4 is also a very good fast ion conductor, its conductivity just above the T_c=575°C is $\sim$3 $ohm^{-1} cm^{-1}$. Anticipating the potential of α-Li_2SO_4 in advanced solid electrolyte batteries and in other electrochemical devices, α-Li_2SO_4 (the high temperature cubic phase) has been extensively studied, for example, the electrical conductivity of pure Li_2SO_4 of various binaries such as Li_2SO_4-$ZnSO_4$, Li_2SO_4-$CaSO_4$, Li_2SO_4-$MgSO_4$, Li_2SO_4-M_2SO_4 where M-is Na,K,Ag,etc, has been studied in detail particularly by Lunden and coworkers (Kvist and Lunden, 1965, Kvist, 1966, Jóseffson and Kvist, 1969, Schroeder et.al., 1972, Aronsson et.al., 1979). However, their all out effort has failed to stabilize the α-Li_2SO_4 disordered-structure at (or near) room temperature, although the conductive to nonconductive

transition temperature (T_c) could be lowered by as much as 100°C, for example, by addition of Na_2SO_4.

Friauf (1976) has shown that all observations involving conductivity and diffusion in the region just below the melting point may be explained as being due to an anomalous rise in the defect concentration caused by a general softening of the lattice. The applicability of α-Li_2SO_4 in practical devices is rather limited as this high conductivity phase is stable only above 575°C.

The low-temperature β-phase has not been studied in any detail. According to Swanson et.al (1968) β-Li_2SO_4 is monoclinic, a = 8.241 Å, b= 4.953 Å c= 8.474 Å and β = 107°58.8'. Shahi et. al (1983) have measured the electrical conductivity of β-Li_2SO_4, and found that it has a conductivity of $\sim 2.5 \times 10^{-6}$ $ohm^{-1} cm^{-1}$ at 300°C and an activation energy of 1.09 eV in the temperature range 280-470°C. Deshpande and Singh (1982) have also studied the conductivity as a function of quenching rates, pressure of pelletization, annealing etc. However, the nature of defects & the mechanisms of conduction etc. are not known as yet.

Following is a discussion of results on Li_2SO_4-LiCl binary which was carried out with a view to obtain a Li_2SO_4-based fast ion conductor at relatively low temperatures, and to shed light on the nature of defects and conduction mechanism in β-Li_2SO_4.

The electrical conductivity of low temperature ($T \lesssim 575$°C) phase of lithium sulphate i.e., β-Li_2SO_4, was measured using a GR 1608A impedence bridge. Predried and premelted materials were used for the conductivity measurements

The variation of electrical conductivity (σ) with inverse of absolute temperature of pure Li_2SO_4 is shown in Fig. 3.1. The observed behavior of conductivity-inverse temperature (σ vs $1/T$) is in accordance with the theory of ionic transport in solids, namely that the conductivity varies exponentially with $1/T$ as given by Eq. (1.5), rewritten below for ready reference .

$$\sigma = n(T)\, e\mu(T) = \sigma_o \exp(-E_a/kT) \quad .. \quad (3.1)$$

where n (T) is the concentration of mobile defects, e their charge, μ (T) their mobility, σ_o the pre-exponential factor, E_a is the overall activation energy for conduction, k the Boltzmann constant, and T the temperature. Thus according to Eq. (3.1), log σ should vary linearly with $1/T$ and the slope of the linear plot should yield the activation energy.

$$\text{Slope} = \frac{E_a}{2.3026\, k}$$

or

$$E_a = -2.3026\, k \times \text{slope (of } \log\sigma \text{ vs. } 1/T \text{)}$$

It is customary to plot log σ vs. $10^3/T$ (rather than log σ vs. $1/T$), and in this case the activation energy E_a is

$$E_a = -2.3026\, k \times 10^3 \times \text{slope (of } \log\sigma \text{ vs. } 10^3/T \text{)}$$

$$E_a(\text{eV}) = -0.1985 \times \text{slope} \qquad (3.2)$$

The intercept of log σ vs. $10^3/T$ plot on log σ- axis gives the exponential factor σ_o. These two parameters, viz., σ_o and E_a, are used to characterize the bulk (macroscopic) conduction properties of solid electrolytes. The calculated values of σ_o and E_a from the linear plots of log σ as a function of inverse

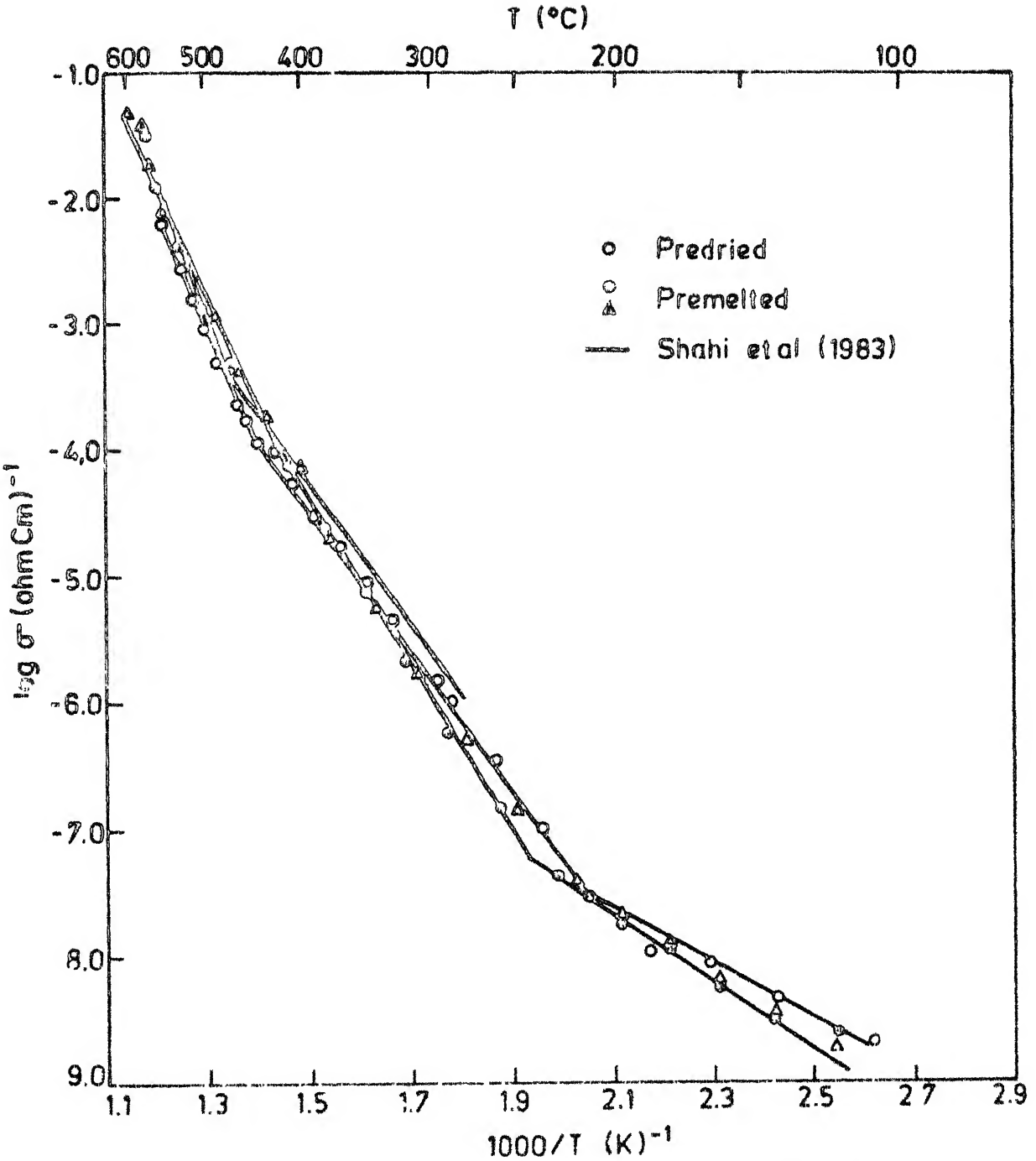

Fig 3.1 Electrical conductivity of pure Li_2SO_4 as a function of temperature

temperature (Fig. 3.1) for β-Li_2SO_4 are given in Table 3.1 which also includes the σ_o and E_a values for other materials studied in this work.

Here we should point out that theoretically it is log (σT) which varies exponentially with $1/T$, and thus log σT vs. $1/T$ should be plotted and used for the calculation of E_a. However, in log (σT) = log σ + log T, the variation of log σ is far greater than that of log T, and therefore the negligence of the term log T hardly makes much difference. It can be illustrated from the following example : Suppose σ varies from 10^{-8} to 10^{-2} ohm^{-1} cm^{-1} corresponding to a change in T from 300 to 800K. Thus while log σ changes by 6, log T changes only by 0.42 which would contribute ~7% to the overall activation energy (say E'_a) obtained from log σ T vs. $1/T$ plot. However, the inconvenience in using log σ T vs. $1/T$ plots is that the approximate conductivity values at desired temperatures can only be known after some calculations. That is rough values of σ cannot be had at the very first look of the plot or figure. For this reason log σ vs. $1/T$ (or $10^3/T$) plots are always preferred and more common in literature. Nevertheless, the log σ T vs. $1/T$ (or $10^3/T$) plots are also sometimes used. The activation energies obtained from these two plots, say E_a and E'_a respectively, are related (Shahi, 1977):

$$E_a = -k \times \text{slope} = -k \frac{\partial(\log \sigma)}{\partial(1/T)} = -k \frac{\partial(\log \sigma)}{\partial x} \quad .. \quad (3.3)$$

and

$$E'_a = -k \times \text{slope} = -k \frac{\partial[\log(\sigma T)]}{\partial(1/T)} = -k \frac{\partial[\log \sigma / x]}{\partial x} \quad .. \quad (3.4)$$

where $x = 1/T$.

Table 3.1

Activation energies and pre-exponential factors for $LiSO_4$-LiCl composites.

Material	σ at T°C ($ohm^{-1}.cm^{-1}$)	Ea(eV)	T-range (°C)	σ_o ($ohm^{-1}cm^{-1}$)
Li_2SO_4	6.25×10^{-3} at 554°C	1.82	440-555	7.65×10^{8}
(predried)	3.08×10^{-5} at 389°C	1.09	215-440	0.61×10^{4}
	4.72×10^{-9} at 139°C	0.42	110-215	0.64×10^{-3}
Li_2SO_4	1.56×10^{-2} at 570°C	1.84	440-600	1.55×10^{9}
(premelted)	0.15×10^{-6} at 260°C	1.29	235-440	2.38×10^{5}
	1.12×10^{-8} at 180°C	0.53	120-235	0.87×10^{-2}
LiCl (predried)	9.04×10^{-6} at 323°C	0.52	90-345	0.22
LiCl (premelted)	3.09×10^{-6} at 340°C	0.73	120-400	3.09
Li_2SO_4+	0.99×10^{-3} at 440°C	1.24	410-600	5.72×10^{5}
10% LiCl	9.70×10^{-5} at 350°C	0.80	290-410	0.28×10^{3}
	3.82×10^{-6} at 260°C	1.50	210-290	5.77×10^{8}
	9.85×10^{-9} at 140°C	0.59	120-210	0.15
Li_2SO_4+	4.84×10^{-3} at 410°C	1.37	240-500	6.17×10^{7}
20% LiCl	0.32×10^{-6} at 210°C	0.75	120-240	2.11
Li_2SO_4+	6.84×10^{-3} at 420°C	1.13	150-500	1.12×10^{-6}
30% LiCl	5.15×10^{-8} at 150°C	0.63	90-150	1.64
Li_2SO_4 +	1.09×10^{-2} at 455°C	1.34	380-500	2.04×10^{7}
40% LiCl	0.25×10^{-3} at 320°C	0.78	250-380	1.07×10^{3}
	0.97×10^{-6} at 199°C	1.42	190-250	1.40×10^{9}
	7.28×10^{-8} at 140°C	0.57	120-190	0.65

Material	σ at T°C (ohm^{-1} cm^{-1})	Ea(eV)	T-range (°C)	σ_o (ohm^{-1} cm^{-1})
Li_2SO_4+	4.23×10^{-3} at 399°C	1.38	360-500	9.40×10^{7}
50% LiCl	3.13×10^{-6} at 180°C	0.60	80-200	1.47
Li_2SO_4 +	1.71×10^{-5} at 315°C	1.18	230-400	2.20×10^{5}
60% LiCl	1.15×10^{-7} at 200°C	0.87	180-230	0.21×10^{3}
	8.20×10^{-9} at 120°C	0.39	100-180	0.82×10^{-3}
Li_2SO_4+	4.48×10^{-5} at 315°C	1.53	295-400	5.77×10^{8}
70% LiCl	4.55×10^{-6} at 270°C	0.95	190-295	2.97×10^{3}
	1.04×10^{-7} at 180°C	0.49	100-190	2.94×10^{-2}
Li_2SO_4 +				
80% LiCl	2.38×10^{-5} at 340°C	1.07	180-400	1.48×10^{4}
	1.05×10^{-8} at 160°C	0.40	100-180	0.47×10^{3}
Li_2SO_4 +				
90% LiCl	3.43×10^{-5} at 340°C	0.87	200-400	0.48×10^{3}
	2.48×10^{-8} at 120°C	0.47	100-200	2.62×10^{-2}

83987

From Eqs. (3.3) and 3.4) we get

$$E'_a - E_a = -k \left[\frac{x}{\sigma} \left(\frac{\partial \sigma}{\partial x} \cdot \frac{1}{x} - \frac{\sigma}{x^2} \right) - \frac{1}{\sigma} \frac{\partial \sigma}{\partial x} \right]$$

or

$$E'_a - E_a = k/x = kT \qquad (3.5)$$

Thus Eq. (3.5) can be readily used to compare the activation energies obtained from either type of plot (Eq. (3.3) or Eq. (3.4)).

It is observed from Table 3.1 and Fig. 3.1 that the conductivity of premelted β-Li_2SO_4 is somewhat higher than that of predried but unmelted β-Li_2SO_4. It is likely to be due to the fact that a fraction of the lattice defects produced at high temperatures on melting is retained on cooling, i.e., the defects generated at high temperature do not get completely anhilated on cooling. If this is the case, then the conductivity enhancement should be a function of quenching rate. The results of Deshpande and Singh (1982) indeed show this tendency to be true, although the effect is not so large.

As for the activation energies, we find three different regions in log σ vs $10^3/T$ plot of Fig. 3.1 associated with E_a = 0.42 eV in the range 110-215°C, 1.09 eV in the range 215-440°C and 1.82 eV in the range 440-555°C. The activation energy in the intermediate temperature range, viz. 1.09 eV in the range 215- 440°C, is in excellent agreement with those of Shahi et.al. (1983) who found the same value in the temperature range 280-470°C. If we level the three regions as I,II and III from high temperature to low, region III may be identified as the one over which the grain-baundary conduction dominates.

The region II may be called the extrinsic-conduction region in which the conduction occurs through diffusion via lattice (bulk conduction) but the mobile lattice defects are introduced by the presence of accidential (aliovalent) impurites, rather than produced as a result of thermodynamic requirement. This region II is therefore impurity controlled extrinsic-region in which the concentration of mobile defects is independent of temperature and is far more than those produced by thermal activation. Thus the activation energy $E_a = 1.09$ eV may be identified as the activation energy for migration (h_m) alone, i.e., in β -Li_2SO_4 E_a (II) = h_m = 1.09 eV (3.6)

The high temperature region "I" between 440 and 555°C is the intrinsic region of conduction. In this temperature range the thermally produced defects outnnumber those present as a result of aliovalent impurities. Thus the overall activation energy E_a(I) should contain both terms i.e.,

$$E_a(I) = \frac{1}{2} h_f + h_m = 1.82 \quad .. \quad (3.7)$$

from Eqs. (3.6) and (3.7) we get

$$h_f = 1.46 \text{ eV} \quad .. \quad .. \quad (3.8)$$

As such the activation energy for the formation of defects in β-Li_2SO_4, i.e., h_f = 1.46 eV sounds reasonable. However, the activation energy for migration h_m = 1.09 eV appears somewhat larger. There are as pointed out earlier, no other published results to compare our data. We therefore tried to look for conduction data on other lithium salts involving divalent anion (e.g., Li_2CO_3, Li_2S, etc.), but they are also not available. The only lithium salts for which data are available are

LiX (X = Cl,Br,I) which exhibit Schottky defects (cation and anion vacancies in equal number). Here it becomes imporant to talk about the nature of defects in Li_2SO_4, that is whether Schottky or Frenkel type of defects are predominant.

In general, an ionic solid such as MX is likely to exhibit Schottky defect if γ_{M^+} and γ_{X^-} are comparable (γ represent the ionic radii). Examples are almost all of the 20 alkali halides. On the other hand, if γ_{M^+} and γ_{X^-} differ considerably, existence of Frenkel defects becomes a possibility. The solid MX may exhibit a cationic or anionic Frenkel disorder depending on whether $\gamma_{M^+} < \gamma_{X^-}$ or $\gamma_{M^+} > \gamma_{X^-}$ respectively. For instance all AgX (X = Cl, Br, I) show predominantly cationic Frenkel disorder while PbF_2,CaF_2 etc. show anionic Frenkel disorder, i.e. F^- interstitials and F^- vacancies. In addition to the size, the net charge on the ion also plays an important role in relation to the nature of defects. Polyvalent (di- , tri- valent) ions are usually immobile in solids for the following reasons. There are two factors,the size and the charge. Smaller the size and charge, of the ion smaller is the energy required to move it. In case of divalent ions, while the size is reduced because of the higher ionisation level to favor its motion, the charge is doubled to increase the activation energy for motion. In general, it is believed that the latter effect (i.e., of charge) is more pronounced than the former, and therefore does not favor the formation and migration of divalent ions. The only exception is O^{2-} which is quite mobile in some oxides (e.g., stabilized Zirconia, CaO. ZrO_2), particularly at high temperatures.

In view of the above discussion, it is quite safe to assume that β-Li_2SO_4 exhibits cationic Frenkel defects, i.e., Li^+- interstitials and vacancies. If we further assume that Li^+ - interstitials are more mobile than Li^+-vacancies, we can identify h_m = 1.09 eV (Eq. 3.6) as the activation energy for migration of Li+ interstitials in β-Li_2SO_4 which is quite large, and indeed unacceptable unless confirmed by other means and measurements.

The data on Li_2SO_4 containing small amounts of LiCl can be used to shed light on the nature of defects. Suppose in β-Li_2SO_4 both interstitials (i) and vacancies (v) are mobile, then the conductivity is given by

$$\sigma = \Sigma\, ne\mu = e\,(\, n_i\, u_i + n_v\, \mu_v\,) \quad .. \quad (3.9)$$

The monovalent Cl^- ion acts as an aliovalent impurity for Li_2SO_4 because the host anion (SO_4^{2-}) is divalent. The substitution of Cl^- in Li_2SO_4 would therefore lead to formation of excess cation vacancies (with an effective negative charge) in order to restore the electrical neutrality of the crystal. Thus the addition of each Cl^- ion would generate a Li-vacancy, and also supress the concentration of Li^+- interstitials because of the mass action law (Lidiard, 1957, Friauf, 1972, Chandra, 1983) which requires that

$$n_i n_V = n_o^2 = \exp\left(-\frac{G_f}{kT}\right) = \text{constant} \qquad (3.10)$$

where $n_o = n_i = n_v$ is the intrinsic concentration of the defects. Now as n_v increases, n_i must decrease in order to make the product $n_i n_v$ constant. Thus for Li_2SO_4+ 10% LiCl sample, one assumes

that only Li^+ vacancies are mobile at lower temperatures, i.e., $n_v \gg n_i$, and that n_v = number of Cl^{-1} ions/ cm^3 = constant, so that Eq. (3.9) reduces to

$$\sigma = e\, n_v\, \mu_v$$

since n_v is constant, a plot of log σ vs. $10^3/T$ should give the activation energy for migration of Li^+-vacancies. The results of Li_2SO_4-10% LiCl are shown in Fig. 3.2. There are four different linear regions associated with E_a (I) = 1.24 eV, E_a(II) = 0.80 eV, E_a(II') = 1.50 eV and E_a (III) = 0.59 eV. If we suppose that E_a (III) is corresponds to grain boundary conduction, then E_a(II') = 1.50 eV should be the activation energy for migration of Li^+-vacancies which is higher than that of Li^+-interstitials as expected.

Then we conclude that our studies indicate that β-Li_2SO_4 exhibits cationic Frenkel defect with Li^+-interstitials being more mobile than Li^+-vacancies. The enthalpy of formation h_f = 1.46 eV, h_m^i = 1.09 eV and h_m^v = 1.50 eV. In view of the fact that h_m^i is rather large considering the small size of Li^+ ions, we suggest that Li_2SO_4 (preferably its single crystals) be further studied to confirm these results. It is worthwhile pointing out here that Aronsson et.al. (1979) from the analysis of neutron diffraction data taken at 20° and 550°C for β-Li_2SO_4 found that there is an increasing freedom of movement for the sulphate ions (SO_4^{2-}). Thus the possibility of Schottky defects at higher temperatures is not completely ruled out, although these authors (Aronsson et.al, 1979) find that the monoclinic phase is crystallographically perfectly ordered, and the space

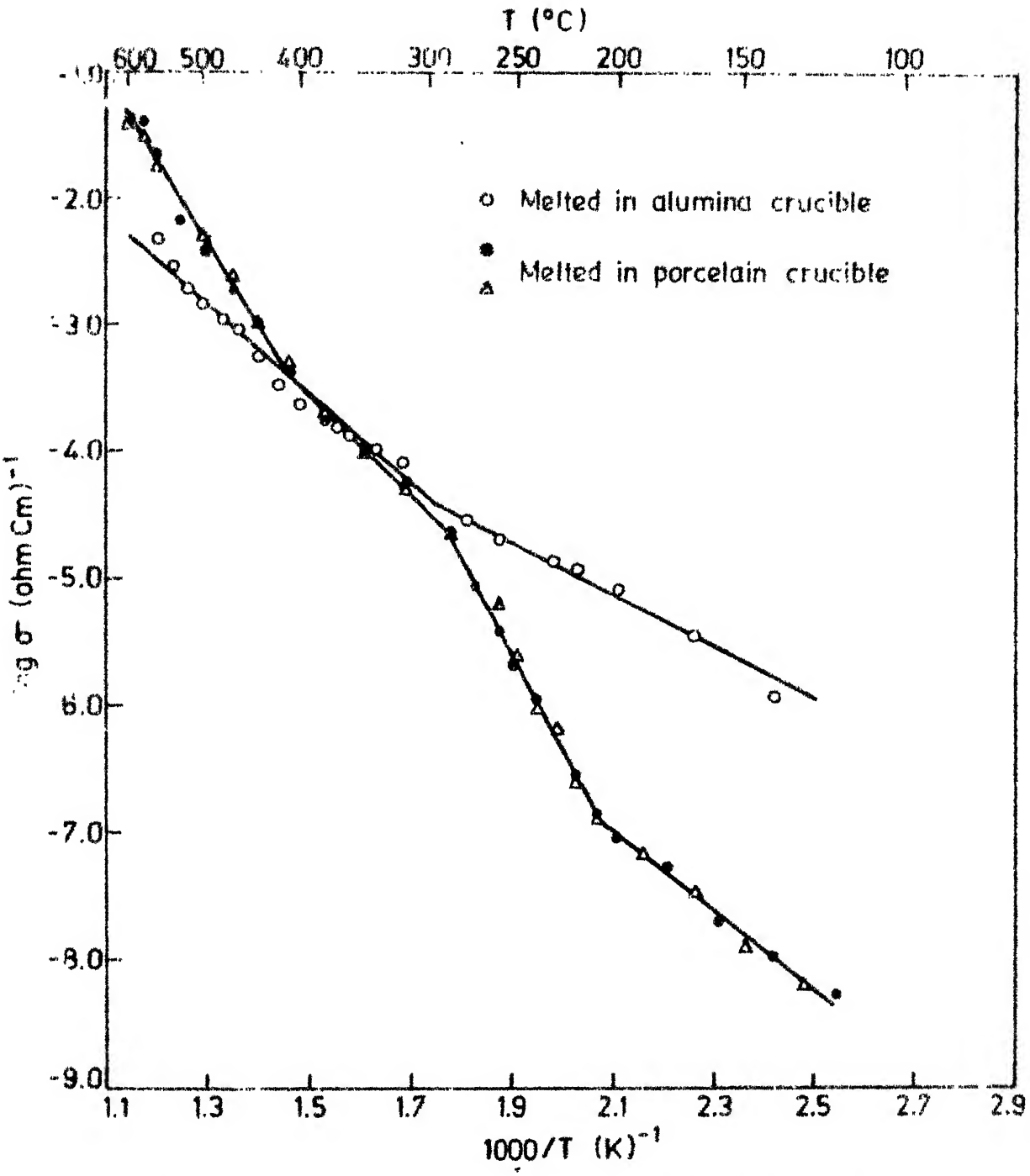

Fig 3.2 Electrical conductivity of 10 mole % LiCl as a function of temperature.

group is retained upto the $\beta - \alpha$ transition temperature(575°C).

In the present investigation, the β to α phase transformation was observed at 571°C, whereas the previous authors (Aronsson et.al, 1979) report T_c = 575°C. The minor discrepancy in T_c is likely to be due to different impurity concentrations in Li_2SO_4 samples, rather than to errors in temperature measurements.

3.1.2 Lithium Chloride

LiCl like other alkali halides, has a rocksalt structure with lattice constant a = 5.129 Å (Wyckoff, 1963). The ionic conductivity in LiCl is attributed to the presence of Schottky defects, i.e. Li^+- and Cl^--ion vacancies. The ionic conductivity of LiCl can therefore be expressed by

$$\sigma = e(n_+ \mu_+ + n_- \mu_-) \quad .. \quad (3.11)$$

where the subscript + and - refer to cation and anion vacancies respectively. In thermodynamic equilibrium

$$n_+ = n_- = n_o \quad .. \quad .. \quad (3.12)$$

where n_o is the concentration of Schottky defects in pure crystal. Since Li^+ ion are much smaller than Cl^- ions, the vacancies of the former are more mobile than Cl^- vacancies i.e., $\mu_+ \gg \mu_-$. Hence

$$\sigma = n_+ e \mu_+ \quad .. \quad .. \quad (3.13)$$

The value of n can be obtained from

$$\frac{n_+}{N} = \exp (Ss/2k). \exp (-H_s/2kT) \quad ..(3.14)$$

where H_s is the enthalpy of formation of a pair of isolated Schottky defects and S_s is the corresponding entropy change. The mobility μ_+ of Li^+ vacancies is given by (Friauf, 1972)

$$\mu_+ = \frac{4e\nu_o a_o^2}{kT} \exp (S_m^+ / k) \exp (-h_m^+/kT) \quad (3.15)$$

where ν_o is the frequency of jump for Li^+ ion , a_o is the cation-anion separation and S_m^+ and h_m^+ correspond to the entropy and enthalpy of migration of Li^+-ion vacancies. The ionic conductivity of predried and premelted lithium chloride (LiCl) has been measured upto temperatures of the order of 400°C. The variation of conductivity versus inverse absolute temperature is shown in Fig. 3.3. Unlike Li_2SO_4, predried LiCl has a higher conductivity and lower activation energy for conduction than those of premelted LiCl sample (see Table 3.1). The differencein the behavior of Li_2SO_4 and LiCl may be due to the basic fact that Li_2SO_4 is less hygroscopic than LiCl. It is possible that the premelted-LiCl sample has less water than the predried-sample, as hence former shows a higher resistivity than the latter. Water is known to increase the conductance of lithium salts.

In log σ vs. $10^3/T$ plot of Fig. 3.3 we observe only one linear region which perhaps corresponds to extrinsic (impurity-dominated) range of conduction, with reference to terminology used for Li_2SO_4, this region may be levelled II. Thus $E_a(II) = h_m^+ = 0.52$ eV for predried LiCl, and 0.73 eV for premelted LiCl. Since we do not observe the intrinsic region (I) whose slope corresponds to ($H_s/2 + h_m$), the formation energy H_s can not be calculated.

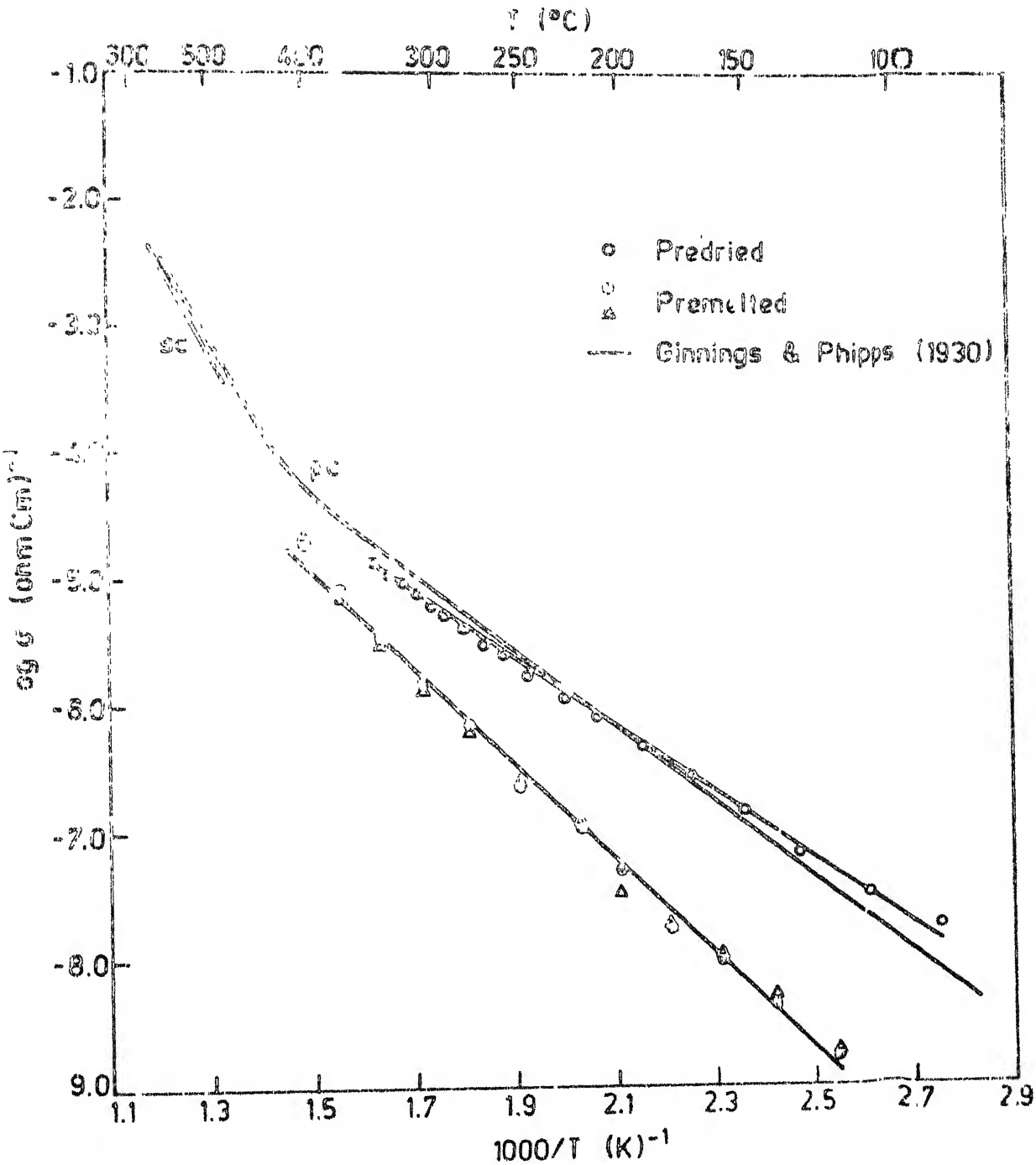

Fig 3.3 Electrical conductivity of pure LiCl as a function of temperature.

LiCl has been studied earlier by Ginnings and Phipps (1930) whose results are also shown in Fig. 3.3. In addition a single crystal study is available after Haven (1950). These studies agree that Li^+ vacancies are the majority charge carriers, i.e., $\mu_+ > \mu_-$. According to Haven (1950), $h_m^+ = 0.41$ eV and $H_s = 2.12$ eV, while Ginnings and Phipps (1930) report an overall activation energy $E_a(I) = 1.42$ eV in the range 400- 500°C and E_a (II) $= h_m^+ = 0.59$ eV. From these data, we get

$$H_s = 2 (E_a - h_m^+) = 1.66 \text{ eV}$$

which is much smaller than the value (2.12 eV) reported by Haven (1950). Our value of $h_m^+ = 0.52$ for the predried LiCl is higher than that of Haven (1950), who of course used single crystals of LiCl, but is closer to that of Ginnings and Phipps (1930) who also employed polycrystalline samples of LiCl.

3. 2 Li_2SO_4-LiCl Composites :

Li_2SO_4-LiCl binary system was examined in an effort to find new Li_2SO_4- based solid electrolyte. LiCl was chosen as additive because the Cl^- ions will act as aliovalent impurity for the host SO_4^{2-} ions, and also because LiCl is one of the lithium salts which do not pose great problems regarding handling, etc.

Fig. 3.4 shows the electrical (ionic) conductivity of Li_2SO_4-LiCl system as a function of composition (mole % LiCl) at three different temperatures, 200°, 300° and 400°C. The conductivity initially increases with increasing concentration of LiCl, peaks around 50 mole% for 200° and 300° C isotherms

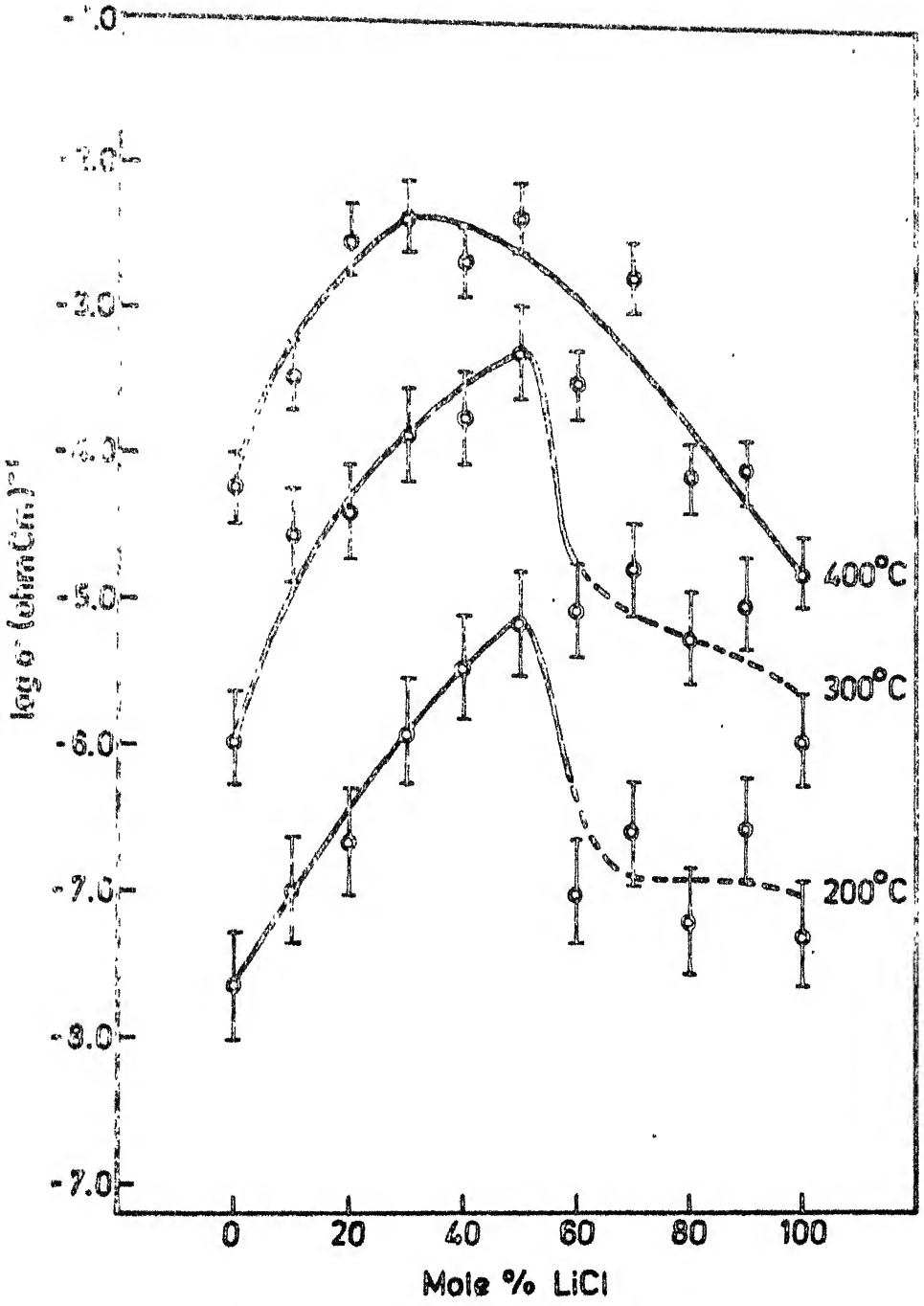

Fig. 3.4 Electrical conductivity variation of Li_2SO_4 - LiCl system with composition at three different temperatures.

and then decreases. The isotherm at 400°C exhibits a peak around 30-35 mole% LiCl, rather than at 50 mole%.

In order to discuss the results of conductivity measurements carried out on composites, a knowledge of phase diagram is desirable. The only phase diagram study of Li_2SO_4-LiCl, we could locate is that of Ljungmark (1974) which is shown in Fig.3.5. Unfortunately the phase diagram is not precisely studied in the low temperature range-the region of our interest, i.e. below 500°C. Also it does not indicate the extent to which solid solutions are formed. As such the phase diagram (Fig. 3.5) does not serve our purpose. We were in fact, interested in working out the Li_2SO_4-LiCl phase diagram at $T < 500°C$ but we could not due to the nonavailability of DTA machine. Also the X-ray diffraction could not be used more than once as it was revealed that Li_2SO_4 tends to attack the sample holder meant for high-temperature X-ray diffraction.

Fig. 3.5 reveals that there is an eutectic at ~60 mole% LiCl (or ~43 mole% Li_2Cl_2) corresponding to the lowest melting point (~ 480°C). The two of the conductivity isotherms (200°C and 300°C) shown in Fig. 3.4 exhibit maxima around 50 mole% LiCl which is close to the eutectic composition (60 mole%) The initial increase in the conductivity of Li_2SO_2-LiCl system (Fig. 3.4) may be due to substitution of Cl^- ions for SO_4^{2-} ions, i.e., due to the formation of solid solution $Li_2SO_{4\ 1-x/2}\ Cl_x$ (where x is mole fraction of LiCl added to Li_2SO_4), as discussed earlier. However, the conductivity of $Li_2SO_{4\ 1-x/2}\ Cl_x$ continues to increas upto x = 0.5. It is highly

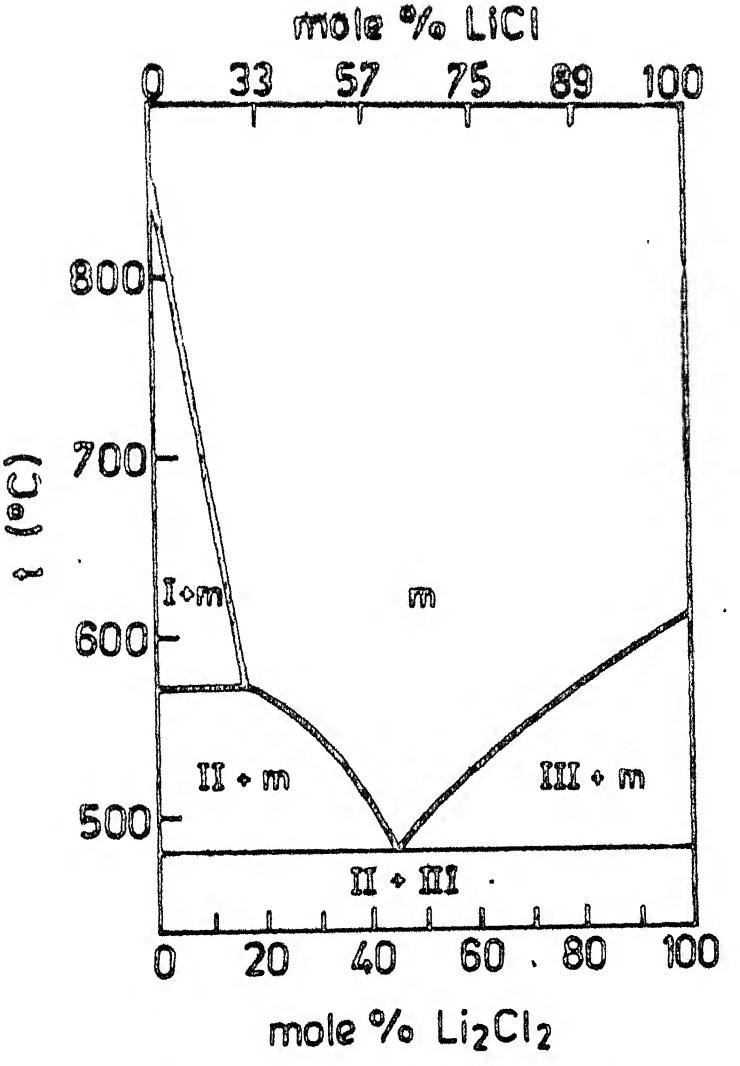

Fig. 3.5 The phase diagram of the system Li_2SO_4 - Li_2Cl_2 (Ljungmark, 1974)

unlikely that Li_2SO_4 would dissolve more than 10 mole% LiCl. Thus the composition range x > 10 mole% LiCl must be a two-phase mixture of Li_2SO_4 containing dissolved LiCl and LiCl containing dissolved Li_2SO_4. It is thus interesting to note that the conductivity of thetwo-phase mixture is greater than the conductivities of either pure phases. It should be recalled here that conductivity enhancements due to second dispersed phase (such as fine Al_2O_3 particles) is reported in case of LiI, AgI, etc. (Liang, 1973, Shahi and Wagner, 1981, 1983). Thus our investigation suggests that the enhancement in the conductivity of two-phase mixtures was not merely limited to Al_2O_3, but was a rather general phenomenon. However, this topic is beyond the scope of this work.

We conclude this part by noting that the Li_2SO_4 containing 50 mole% LiCl exhibits almost 100 times higher conductivity than pure Li_2SO_4, its conductivity being 4×10^{-3} $ohm^{-1} cm^{-1}$ at 400°C. An unexplained feature of Fig. 3.5 is the shifting of maximum towards left (i.e. lower concentration of LiCl) at higher temperatures.

Fig. 3.6 shows the conductivity of Li_2SO_4-LiCl system as a function of temperature for 11 different compositions at a regular interval of 10 mole% . Fig. 3.7 and 3.8 show the same results for fewer compositions at an interval of 20 mole% for the sake of clarity. The conduction data, i.e., the pre-exponential factor σ_o and the activation energy E_a, for all compositions are summarized in Table 3.1.

As such the results are quite involving, and perhaps a quantitative discussion is not possible. However, we shall mention

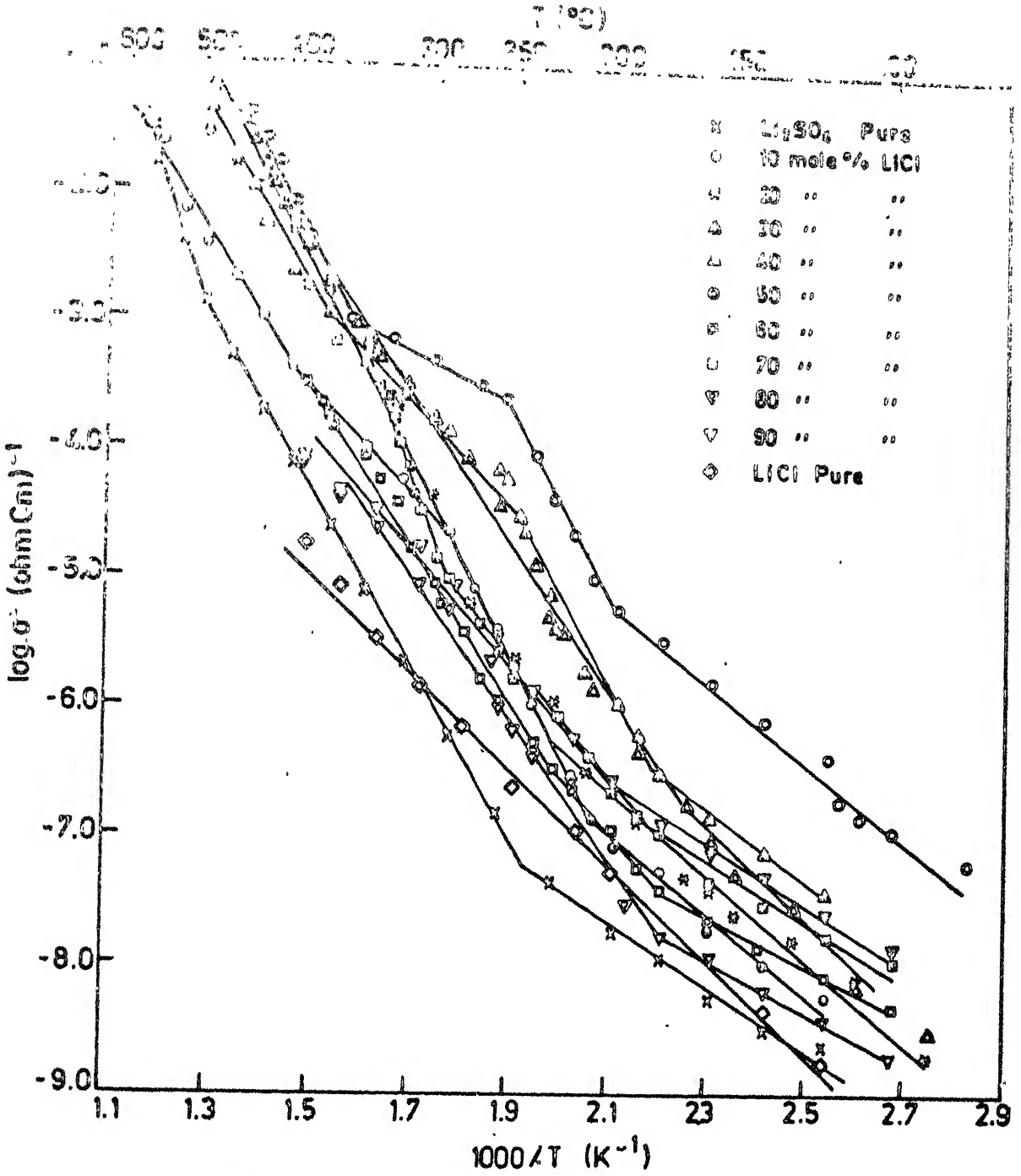

Fig. 3.6 Electrical conductivity variation of various compositions of Li_2SO_4 - LiCl with temperature.

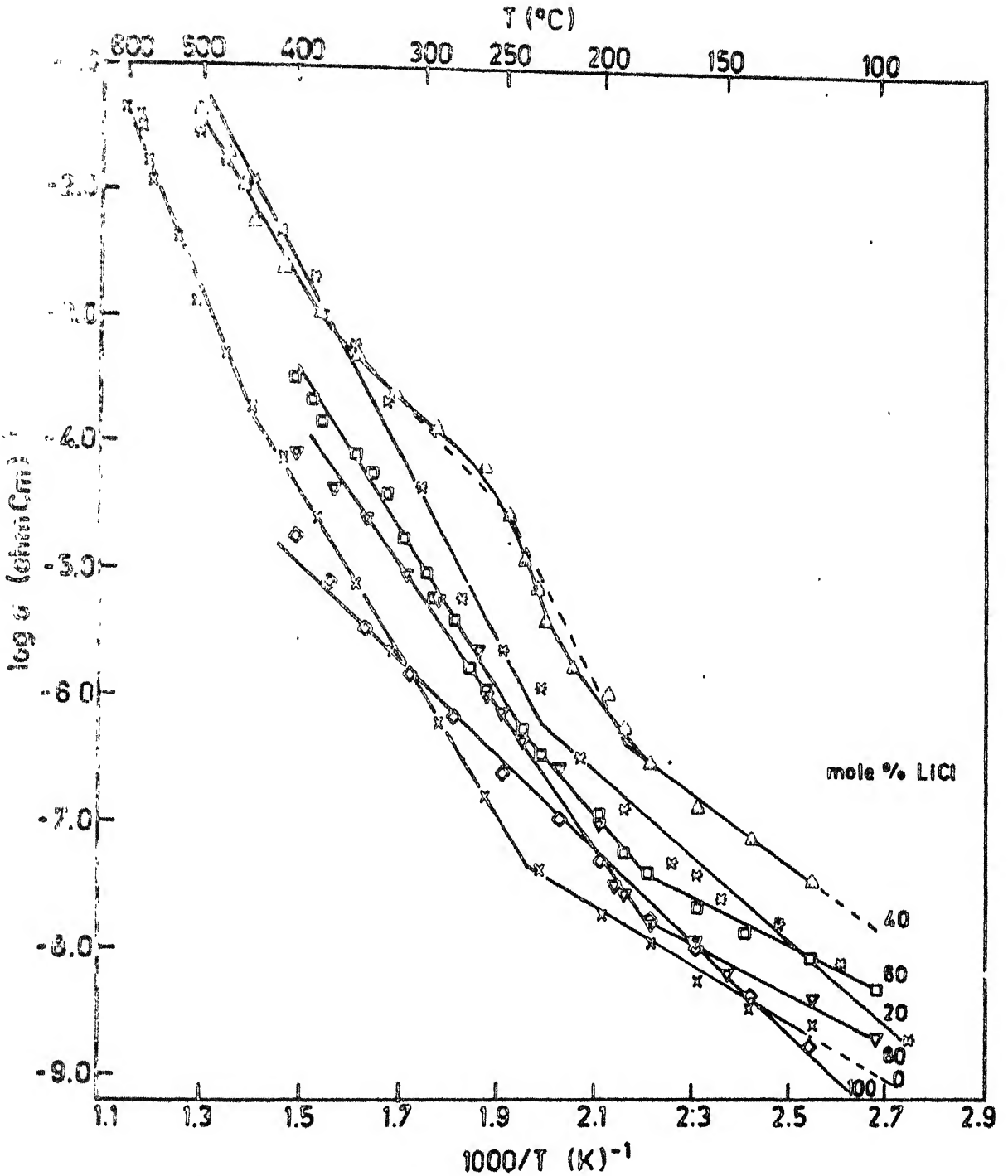

Fig. 3.7 Electrical conductivity variation of even compositions of Li_2SO_4 - LiCl with temperature.

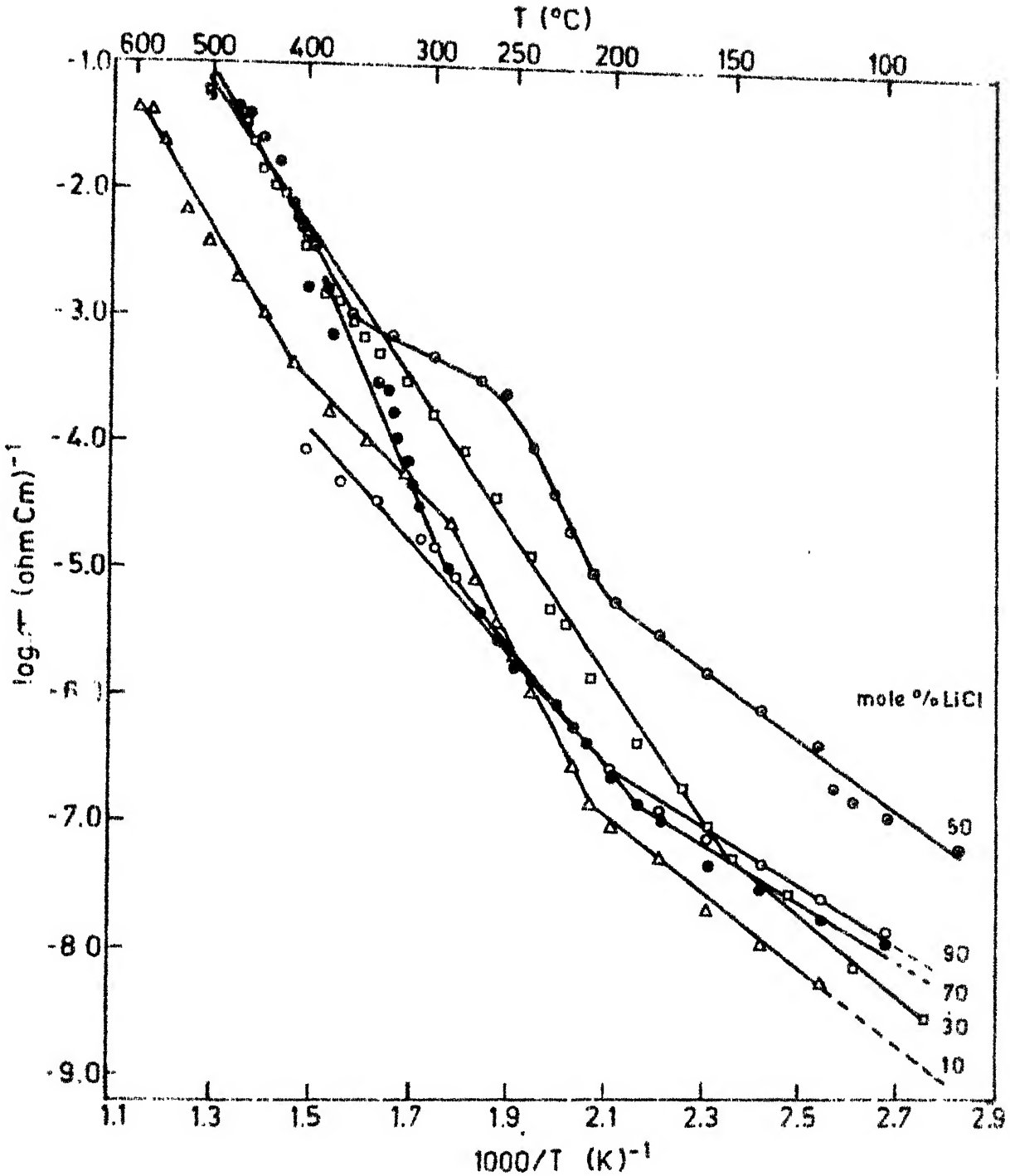

Fig 3.8 Electrical conductivity variation of odd compositions of Li_2SO_4 - LiCl with temperature.

only some of the broad features. It is seen from Figs. 3.6 and 3.8 that the composition corresponding to highest conductivity, i.e., 50 mole% LiCl, shows a sort of nonlinear behavior in the intermediate temperature range 230°-350°C. This should suggest that ratio of the mole fraction of the two solid solution (ss) phases, namely Li_2SO_4 ss and LiCl ss, is changing with temperature, and thus different activation energies are involved.

The slopes of the lowest temperature region for all the Li_2SO_4-rich compositions are nearly same, around 0.60 eV, which appears to correspond with the grain boundary conduction. Similarly, for all the LiCl-rich compositions, the activation energy in low T-region is 0.40-0.47 eV, close to the value of LiCl-pure.

The conductivity-temperature dependence for each of the 9 composites is shown separately in Figs. 3.9 to 3.16.

The conductivity temperature dependence of Li_2SO_4 + 10 mole % LiCl is already shown in Fig. 3.2. A notable feature of the log σ vs. $1/T$ plot for this composition is that it consists of four linear segments, rather than three as observed for pure Li_2SO_4. The conductivity-temperature dependence can be described by the following equations.

$$\sigma = 0.15 \exp\left(-\frac{0.59\ eV}{kT}\right) \qquad 120° - 210°C$$

$$\sigma = 5.77 \times 10^{8} \exp\left(-\frac{1.50\ eV}{kT}\right) \qquad 210 - 290°C$$

$$\sigma = 2.8 \times 10^{2} \exp\left(-\frac{0.80\ eV}{kT}\right) \qquad 290 - 410°C$$

$$\sigma = 5.7 \times 10^{5} \exp\left(-\frac{1.24\ eV}{kT}\right) \qquad 410 - 600°C$$

One extra linear region in case of Li_2SO_4 doped with 10 mole% LiCl may be due to association of impurity atoms with vacancies, or precipitation of impurites as the temperature is lowered.

Fig. 3.9 shows the conductivity-temperature variation for Li_2SO_4 + 20 mole% LiCl. Im sharp contrast to 10 mole% LiCl composition (Fig. 3.2), 20 mole% composite shows only two linear segments which can be described by

$$\sigma = 2.11 \exp\left(-\frac{0.75\ eV}{kT}\right) \qquad 120 - 240°C$$

and

$$\sigma = 6.17 \times 10^{7} \exp\left(-\frac{1.37\ eV}{kT}\right) \qquad 240 - 500°C$$

The reason for sharp difference between the two samples can only be explained if the precise phase diagram was available.

Fig. 3.10 shows the same results for Li_2SO_4 + 30 mole% LiCl. This sample also exhibits only two linear regions which can be expressed by

$$\sigma = 1.64 \exp\left(-\frac{0.63\ eV}{kT}\right) \qquad 90 - 150°C$$

and

$$\sigma = 1.12 \times 10^{6} \exp\left(-\frac{1.13\ eV}{kT}\right) \qquad 150 - 500°C$$

In contrast to 20 or 30 mole% LiCl the conductivity-temperature variation of Fig. 3.11 for Li_2SO_4 + 40 mole% LiCl

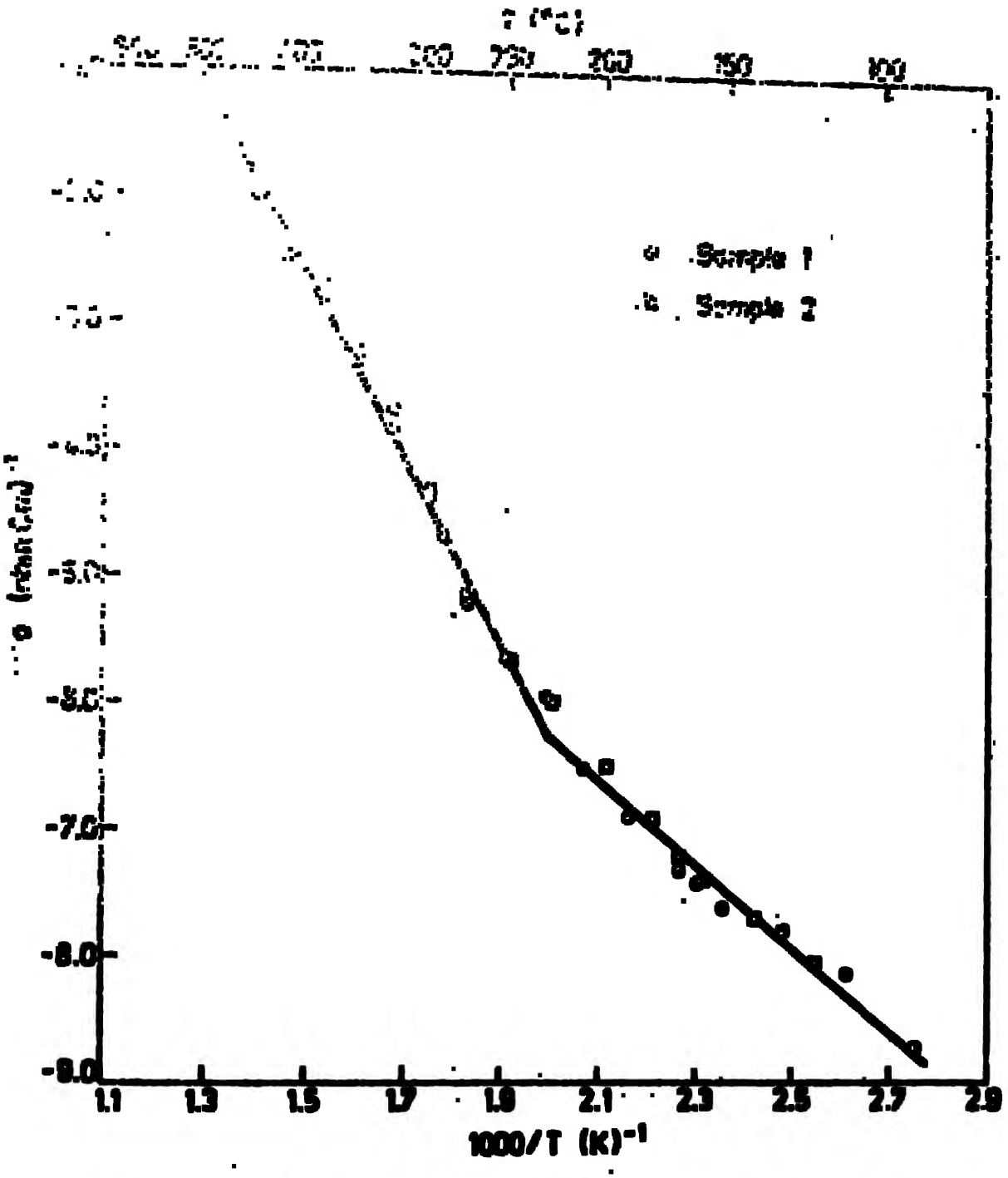

Fig. 3.9 Electrical conductivity of 20 mole % LiCl as a function of temprature.

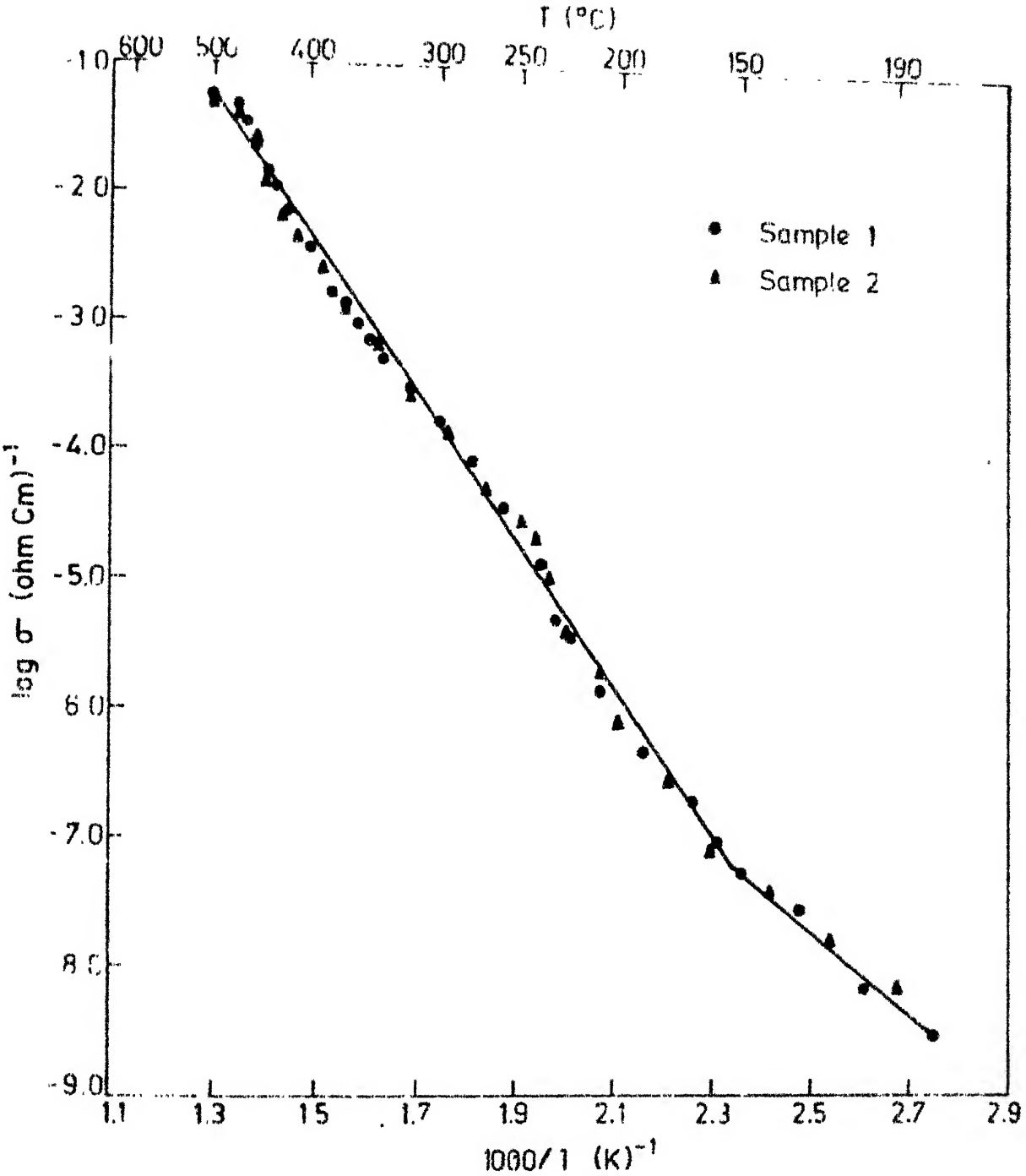

Fig 3.10 Electrical conductivity of 30 mole % LiCl as a function of temperature.

has four linear regions which can be expressed by

$$\sigma = 0.65 \exp\left(-\frac{0.57\ eV}{kT}\right) \qquad 120 - 190°C$$

$$\sigma = 1.4 \times 10^{9} \exp\left(-\frac{1.42\ eV}{kT}\right) \qquad 190 - 250°C$$

$$\sigma = 1.07 \times 10^{3} \exp\left(-\frac{0.78\ eV}{kT}\right) \qquad 250 - 380°C$$

$$\sigma = 2.04 \times 10^{7} \exp\left(-\frac{1.34\ eV}{kT}\right) \qquad 380 - 500°C$$

The plot of Fig. 3.12 for Li_2SO_4 + 50 mole% LiCl has three regions. The low and high temperature regions are linear and the intermediate temperature region is non-linear and has a curved slope. This composition has the highest conductivity of the system. The conductivity in the low and high temperature regions varies with temperature as

$$\sigma = 1.47 \exp\left(-\frac{0.60\ eV}{kT}\right) \qquad 80 - 200°C$$

$$\sigma = 9.4 \times 10^{7} \exp\left(-\frac{1.38\ eV}{kT}\right) \qquad 360 - 500°C$$

The three regions of the Fig. 3.13 for Li_2SO_4 + 60 mole% LiCl can be expressed as

$$\sigma = 0.82 \times 10^{-3} \exp\left(-\frac{0.39\ eV}{kT}\right) \qquad 100 - 180°C$$

$$\sigma = 0.21 \times 10^{3} \exp\left(-\frac{0.87\ eV}{kT}\right) \qquad 180 - 230°C$$

$$\sigma = 2.2 \times 10^{5} \exp\left(-\frac{1.18\ eV}{kT}\right) \qquad 230 - 400°C$$

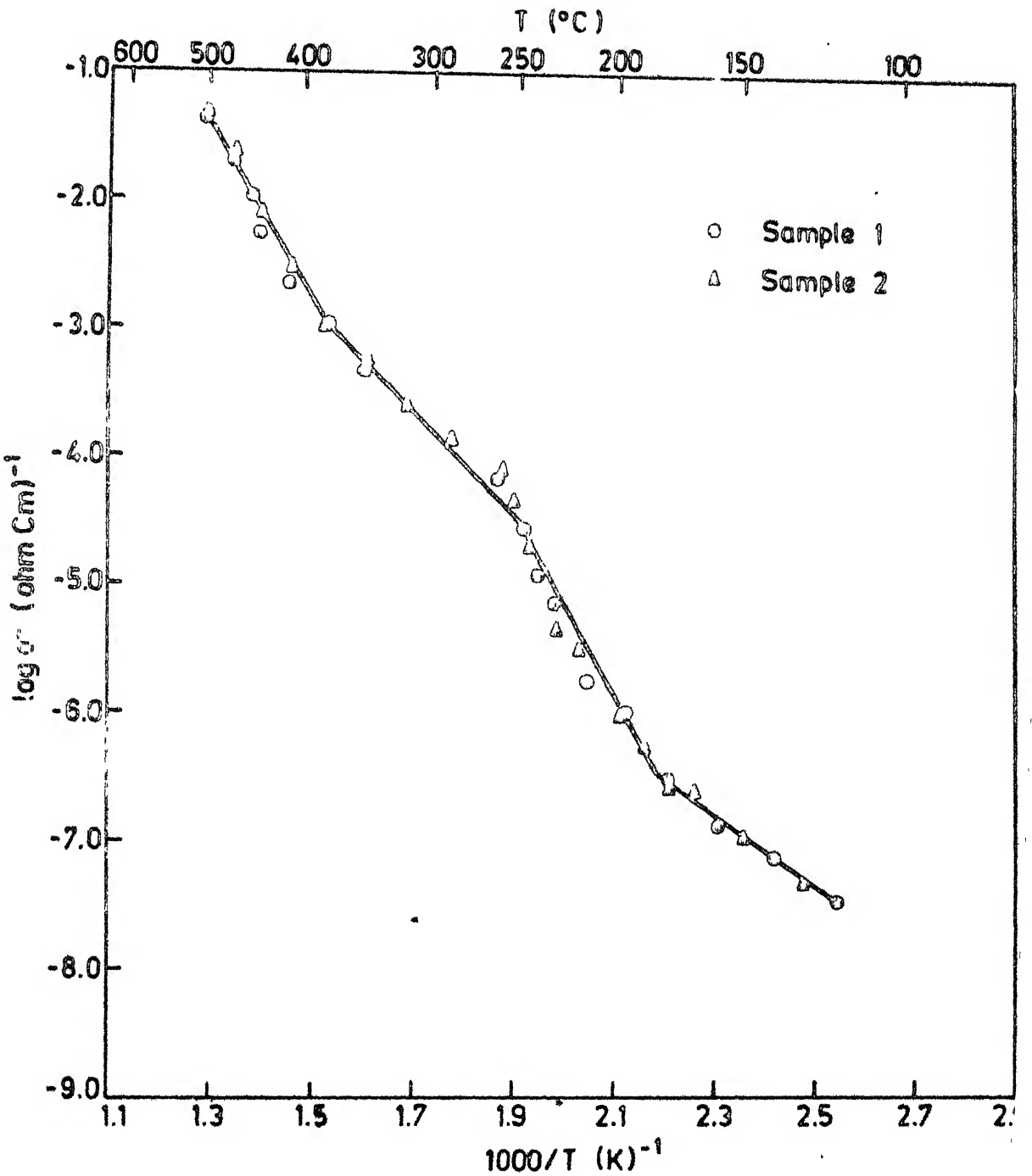

Fig. 3.11 Electrical conductivity of 40 mole % LiCl as a function of temperature.

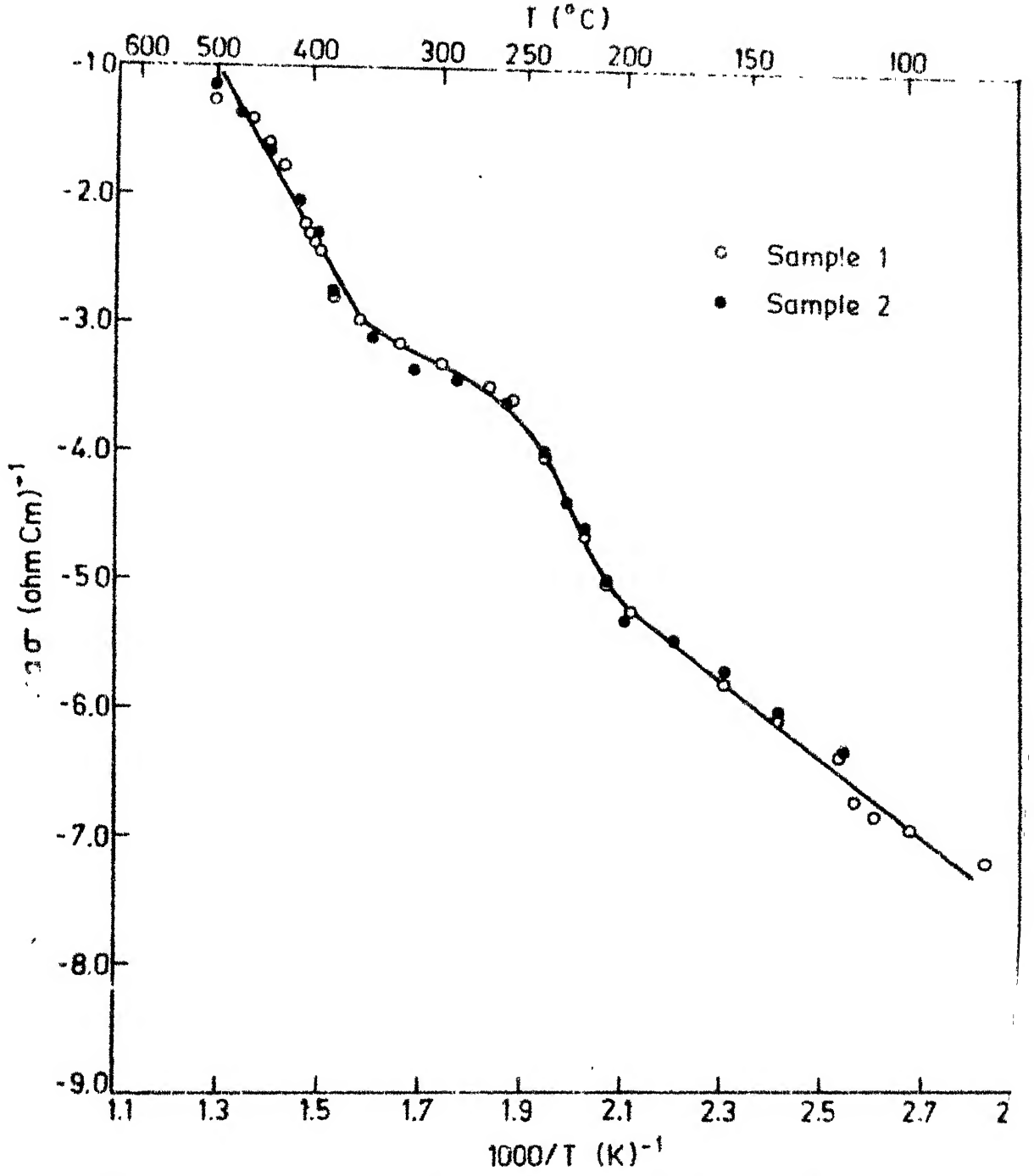

Fig. 3.12 Electrical conductivity of 50 mole% LiCl as a function of temperature.

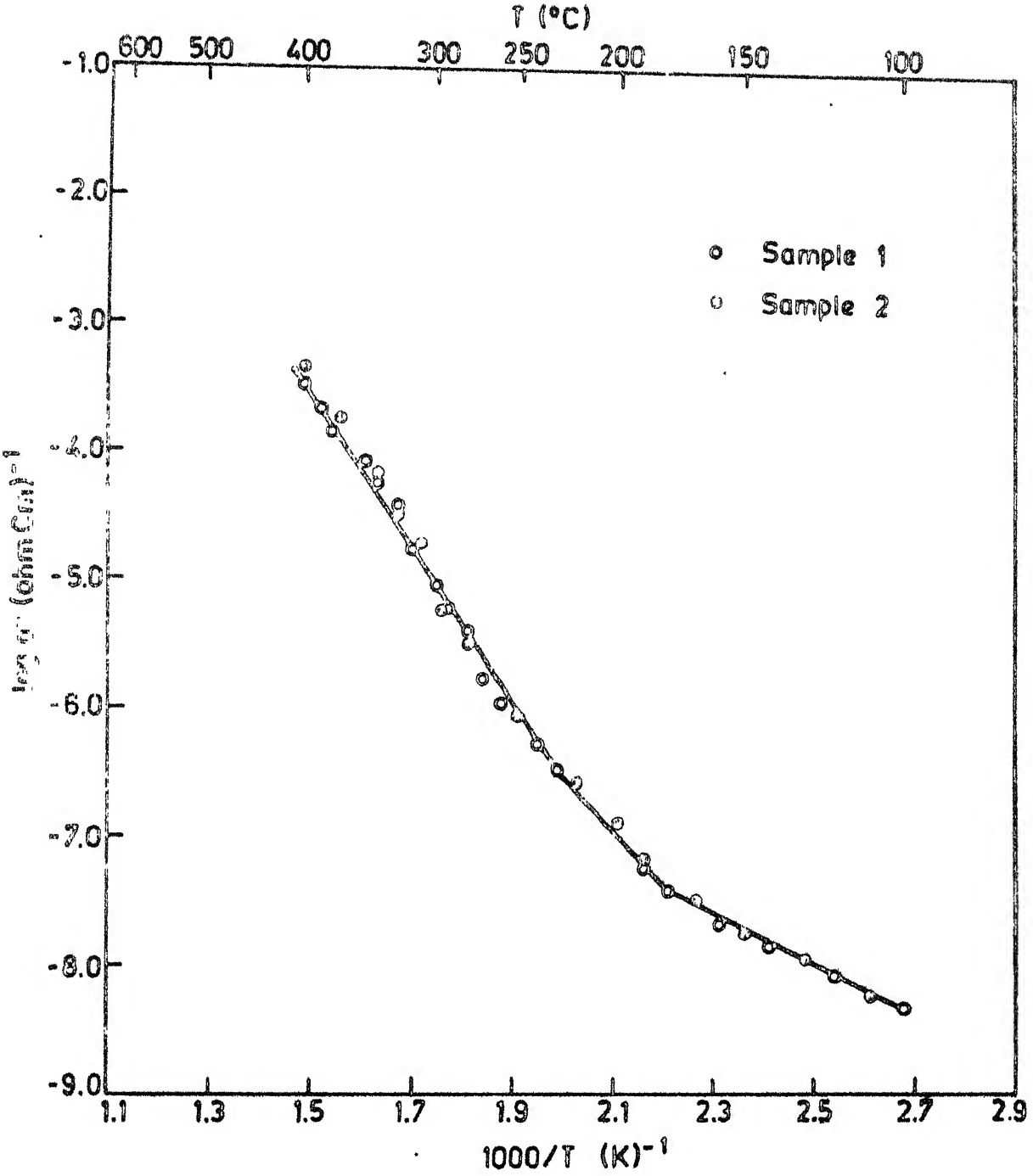

Fig. 3.13 Electrical conductivity of 60 mole% LiCl as a function of temperature.

Similarly various linear regions of figures (3.14), (3.15) and (3.16) respectively for $LiSO_4$ containing 70,80 and 90 mole percents can be described as follows

for Li_2SO_4 + 70 mole% LiCl,

$$\sigma = 2.94 \times 10^{-2} \exp\left(-\frac{0.49\ eV}{kT}\right) \qquad 100 - 190°C$$

$$\sigma = 2.97 \times 10^{3} \exp\left(-\frac{0.95\ eV}{kT}\right) \qquad 190 - 295°C$$

$$\sigma = 5.77 \times 10^{8} \exp\left(-\frac{1.53\ eV}{kT}\right) \qquad 295 - 400°C$$

for Li_2SO_4 + 80 mole% LiCl,

$$\sigma = 0.47 \times 10^{-3} \exp\left(-\frac{0.40\ eV}{kT}\right) \qquad 100 - 180°C$$

$$\sigma = 1.48 \times 10^{4} \exp\left(-\frac{1.07\ eV}{kT}\right) \qquad 180 - 400°C$$

and for Li_2SO_4 + 90 mole% LiCl,

$$\sigma = 2.62 \times 10^{-2} \exp\left(-\frac{0.47\ eV}{kT}\right) \qquad 100 - 200°C$$

$$\sigma = 0.48 \times 10^{3} \exp\left(-\frac{0.87\ eV}{kT}\right) \qquad 200 - 400°C$$

3.3 Li_2SO_4- LiCl- Al_2O_3 SYSTEM

According to literature electrical conductivity of various solid electrolytes can be enhanced by the addtion of fine Al_2O_3 particles. Liang (1973,1978) found that the ionic conductivity of LiI could be increased by 2-3 orders of magnitude by a dispersion

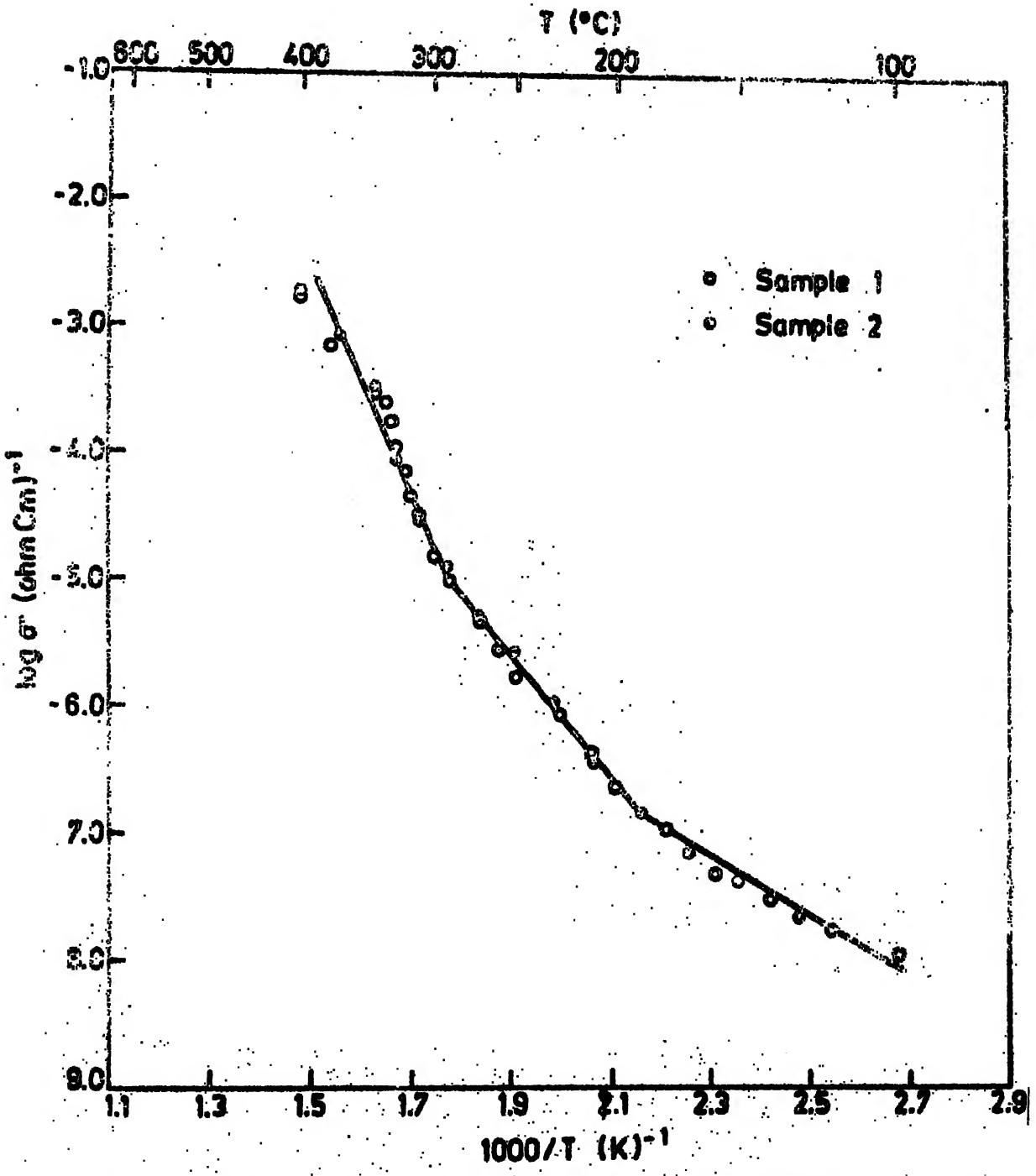

Fig. 3.14 Electrical conductivity of 70 mole % LiCl as a function of temperature.

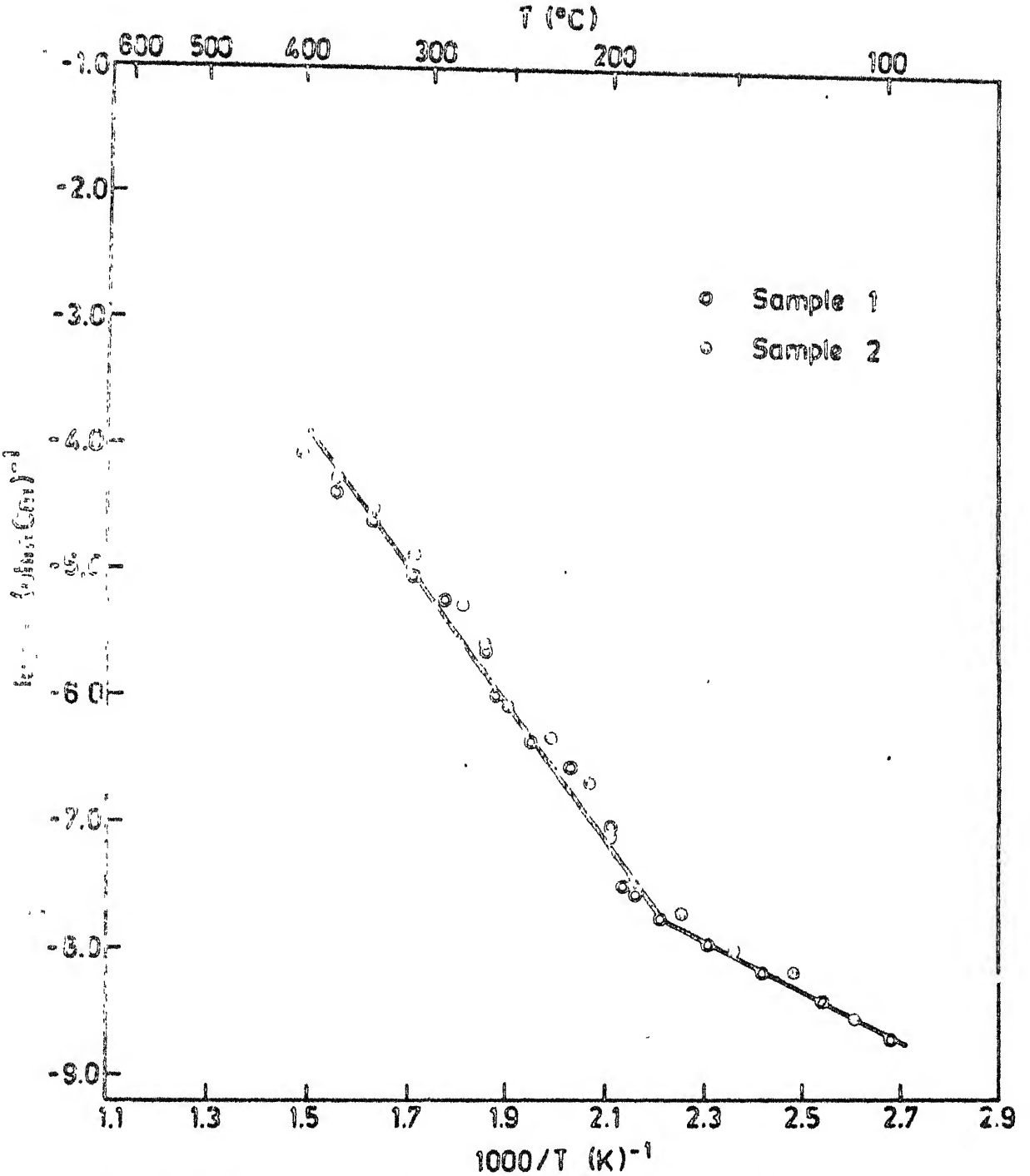

Fig. 3.15 Electrical conductivity of 80 mole% LiCl as a function of temperature

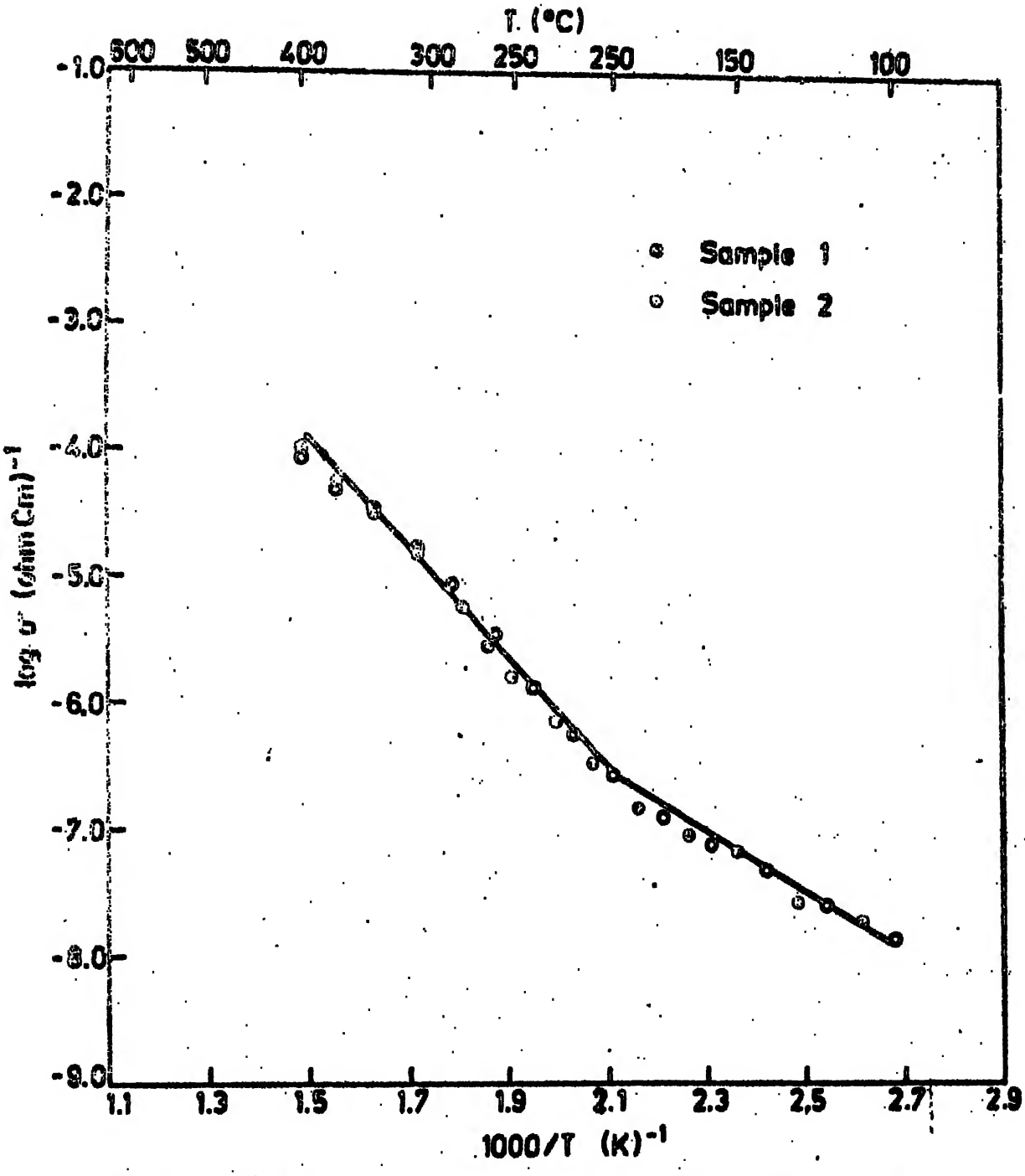

Fig. 3.18 Electrical conductivity of 90 mole % LiCl as a function of temperature.

of 40 to 50 mole% Al_2O_3 at room temperature. This enhancement in conductivity of solid electrolytes by fine dispersoids was found by Shahi and Wagner (1981) to be a general phenomenon. They reported enhanced conductivity in AgI-Al_2O_3, AgI-SiO_2, AgI-AgBr, AgI- flyash etc. by a factor ranging from 50-1000. In view of these reports, it was felt worthwhile measuring the conductivity of Li_2SO_4-LiCl system containing Al_2O_3 particles.

Li_2SO_4 - 30 mole% LiCl mixture was taken and to this 30 mole Al_2O_3 (particle size 0.05 μm) was added. The materials were weighed accurately (as described earlier in § 2.1), mixed thoroughly in agate mortar and pestle and heated to ~1000°C for about 4 hours in a porcelain crucible. The air-quenched material was finely ground and pellet made as discussed in Chapter 2. The sample was annealed at ~400°C for about 5 hours and electrical conductivity was measured as a function of temperature during the cooling cycle. The results are shown in Fig. 3.17. Suprisingly the conductivity was found to decrease with the addition of Al_2O_3 by a factor of 40 at higher temperatures. However, the decrease was less at temperatures ≤200°C. It is possible that some enhancement in conductivity may be observed at temperatures below 80°C, but we could not cover this low temperature range.

3.4 SUMMARY AND CONCLUSIONS

β-Li_2SO_4 appears to exhibit cationic Frenkel defects (i.e., Li^+-interstitials and Li^+- vacancies). The energy of formation (H_f) is found to be 1.46 eV. The activation energy for the migration of more mobile Li^+- interstitials is 1.09 eV.

The conductivity of Li_2SO_4 could be increased by a factor

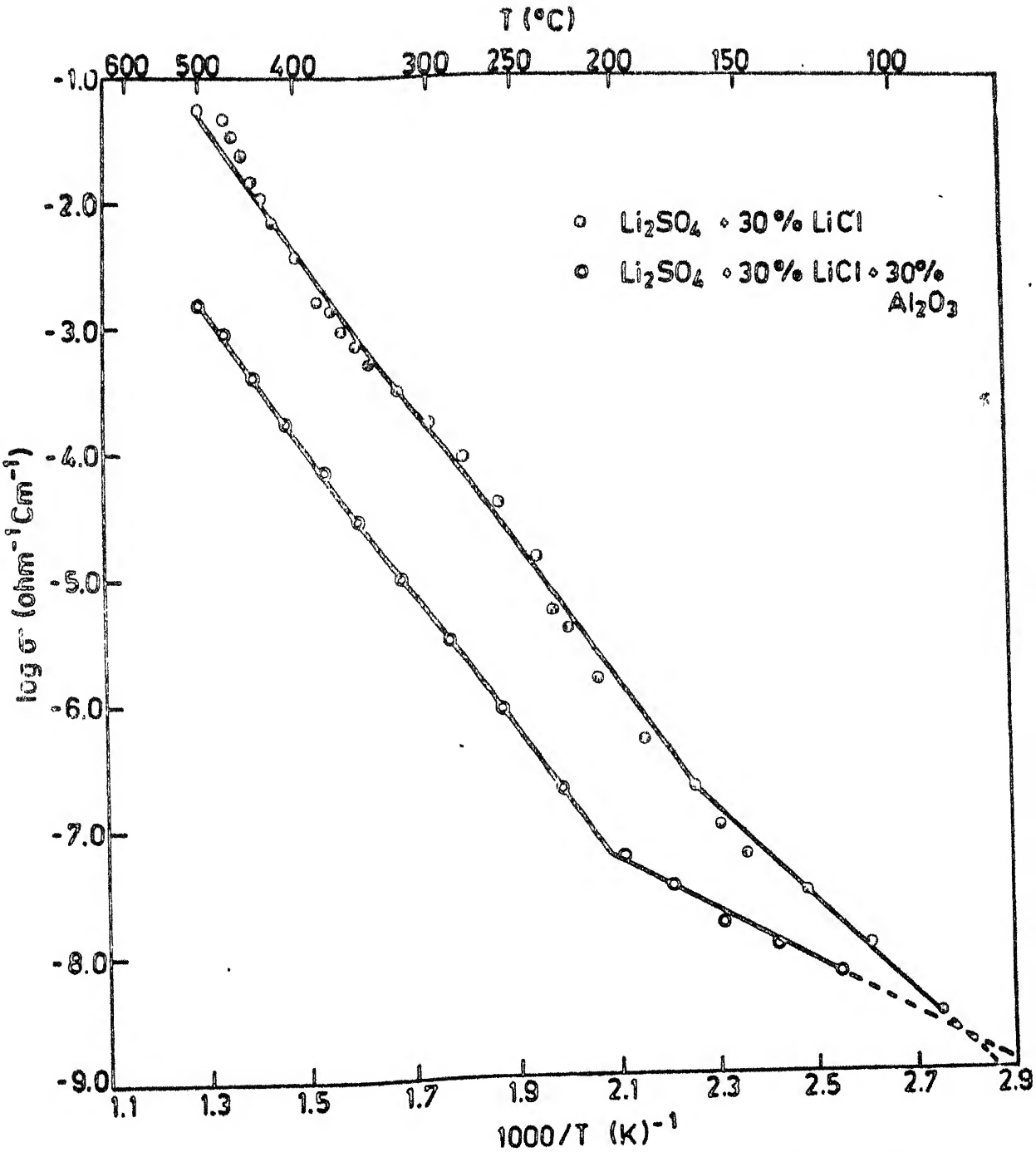

Fig. 3.17 Electrical conductivity variation of Li_2SO_4 + 30% LiCl + 30% Al_2O_3 with temperature..

of 1000 by adding 50 mole % LiCl at temperature of 200-400°C, and by a factor of 50 at temperatures above 400°C. The defect structure and conduction mechanism in Li_2SO_4-LiCl composites is not very clear in absence of the phase diagram below 500°C. The mixtures exhibiting high conductivity also show a lower activation energy for conduction which is consistent. The best conducting composition (viz., Li_2SO_4-50 mole% LiCl) has a conductivity $\sim 5.5 \times 10^{-2}$ $ohm^{-1} cm^{-1}$ at 500°C which may be used in high temperature batteries and fuel cells.

Dispersion of fine Al_2O_3 particles in Li_2SO_4-40 mole% LiCl has not shown any further improvement in the conductivity.

The conduction parameters (pre-exponential factor and activation energy) for 11 compositions of Li_2SO_4- x LiCl (x= 0,0.1,0.2,0.3,0.4,0.5,0.6,0.7,0.8,0.9,1.0) are calculated from the experimental data (log σ vs. 1/ T plots) and summarized in Table 3.1.

REFERENCES

1. Alpen, U.V. and Bell, M.F., in "Fast Ion Transport in Solids", eds. Vashishta, P., Mundy, J.N. and Shenoy, G.K., North-Holland, Elsevier (1979), p.463.
2. Aronsson,R., Heed, B., Jonsson, B., Lunden, A., Nilsson, L., Schroeder, K., and Sjoblom C.A., in "Fast Ion Transport in Solids", eds. Vashishta, P., Mundy. J.N. and Shenoy, G.K., North Holland,Elsevier (1979), pp. 471-474.
3. Barak, M., "Proc. IEE.", 117, 1561 (1970).
4. Barak, M., "Electronics and Power", 18, 290 (1972).
5. Cairns, E.J. and Shimotake, H., "Seience", 164, 1347 (1969).
6. Chandra, S., in "Superionic Solids", North-Holland, Amsterdam (1982).
7. Choudhary, C.B., Maiti, H.S., and Subba Rao, E.C., in "Solid Electrolytes and Their Applications", ed. Subba Rao, E.C., Plenum Press, New York (1980).
8. Debasis Baral, M.Tech. Thesis, IIT, Kanpur (1974).
9. Deshpande, V.K. and Singh, K., "Solid State Ionics", 6, 151 (1982).
10. Deshpande, V.K. and Singh, K., "Solid State Ionics", 7, 295 (1982).
11. Deshpande, V.K. and Singh, K., "Solid State Ionics", 8, 319 (1983).
12. Deshpande, V.K. and Singh, K., "J. Power Sources", 10, 191 (198
13. Forland, T. and Krogh-Moe, J., "Acta Chem.Scand", 11, 565 (1957
14. Friauf, R.J., in "Physics of Electrolytes", Vol. 1, ed Hladik,J Academic Press, London (1972).
15. Friauf, R.J., "J. Phys. Coll", 37, C-7 393 (1976).
16. Geller, S., in "Solid Electrolytes", ed. Geller,S, Springer-Verlag, Berlin (1977).

17. Goodenough, J.B., in "Solid Electrolytes", ed. Geller, S., Springer-Verlag, Berlin (1977)., p. 394.

18. Hagenmuller, P. and Van Gool, W., in "Solid Electrolytes", eds. Hagenmuller, P., and Van Gool, W., Academic Press, New York (1978), pp. 536-538, 543.

19. Haven, Y., "Rec. Trav. Chim", 69, 1471 (1950).

20. Heed, B., Lunden, A., and Schroeder, K., "Electrochimica Acta" , 22, 705 (1977).

21. Hladik, J., in "Physics of Electrolytes", Vol. 1, ed., Hladik, J., Academic Press, London (1972) p. 36.

22. Huggins, R.A., " Electrochimica Acta", 22, 773 (1977).

23. Jagannathan, K.P., Tiku, S.K., Ray, H.S., Ghosh,A., and Subba Rao,E.C., in "Solid Electrolytes and Their Applications", ed. Subba Rao, E.C., Plenum Press, New York (1980).

24. Josefson, A.M., and Kvist, A., "Z. Naturforsch", 24a, 466 (1969).

25. Josefson, A.M., and Kvist, A.," Z. Naturforsch", 25a 1917 (1970).

26. Kennedy, J.H., in " Solid Electrolytes", ed. Geller, S., Springer-Verlag, Berlin (1977).

27. Kvist, A., " Z. Naturforsch", 20a, 235 (1965).

28. Kvist, A., " Z. Naturforsch", 21a , 487 (1966).

29. Kvist, A., " Z. Naturforsch", 21a , 1121 (1966).

30. Kvist, A., "Z. Naturforsch"., 21a , 1601 (1966).

31. Leif Nilsson, Thesis, University of Gothenburg (1981).

32. Liang, C.C., "J. Electrochem. Soc"., 120, 1289 (1973).

33. Liang, C.C., Joshi, A.V., and Hamilton, N.T., "J. Appl. Electronchem.", 8 , 445 (1978).

34. Lidiard, A.B., in" Encyclopedia of Physics", ed. Flugge,S., Vol. XX, Springer-Verlag, Berlin, p. 246.

35. Ljungmark, H., Thesis, University of Gothenburg (1974).

36. Owens, B.B. and Skarstand, P.M., in" Fast Ion Transport in Solids", eds. Vashishta,P., Munday, J.N., and Shenoy, G.K., North-Holland, Elsevier (1979) pp. 61-66.

37. Rice, M.J. and Roth, W.L., "J. Solid State Chem"., 4, 294 (1972).

38. Salamon, M.B., in" Physics of Superionic Conductors", ed. Salamon,M.B., Springer-Verlag, Berlin (1979) pp. 1-3.

39. Sato, H., in "Solid Electrolytes", ed., Geller, S., Springer-Verlag, Berlin (1977).

40. Schroeder, K., Kvist, A., and Ljungmark, H., "Z. Naturforsch", 27a , 1252 (1972).

41. Shahi, K., "Phys. Stat. Solidi A41, 11 (1977).

42. Shahi, K. and Wagner, J.B., Jr. " J. Solid State Chem.", 42, 107 (1982).

43. Shahi, K., Wagner, J.B., and Owens, B.B., in " Lithium Batteries", ed. Gabano, J.P., Academic Press, London (1983).

44. Shannon, R.D., Taylor, B.E., English, A.D., and Berzins, T., " Electrochimica Acta", 22, 783 (1977).

45. Swanson, H.E., Mc Murdie, H.F., Morris, M.C., and Evans, E.H., " NBS monograph" (1968).

46. Wyckoff, R.W.G., " Crystal Structures", 2nd edition, Vol. I and II, Interscience, New York (1963).